

this document downloaded from

# vulcanhammer.info

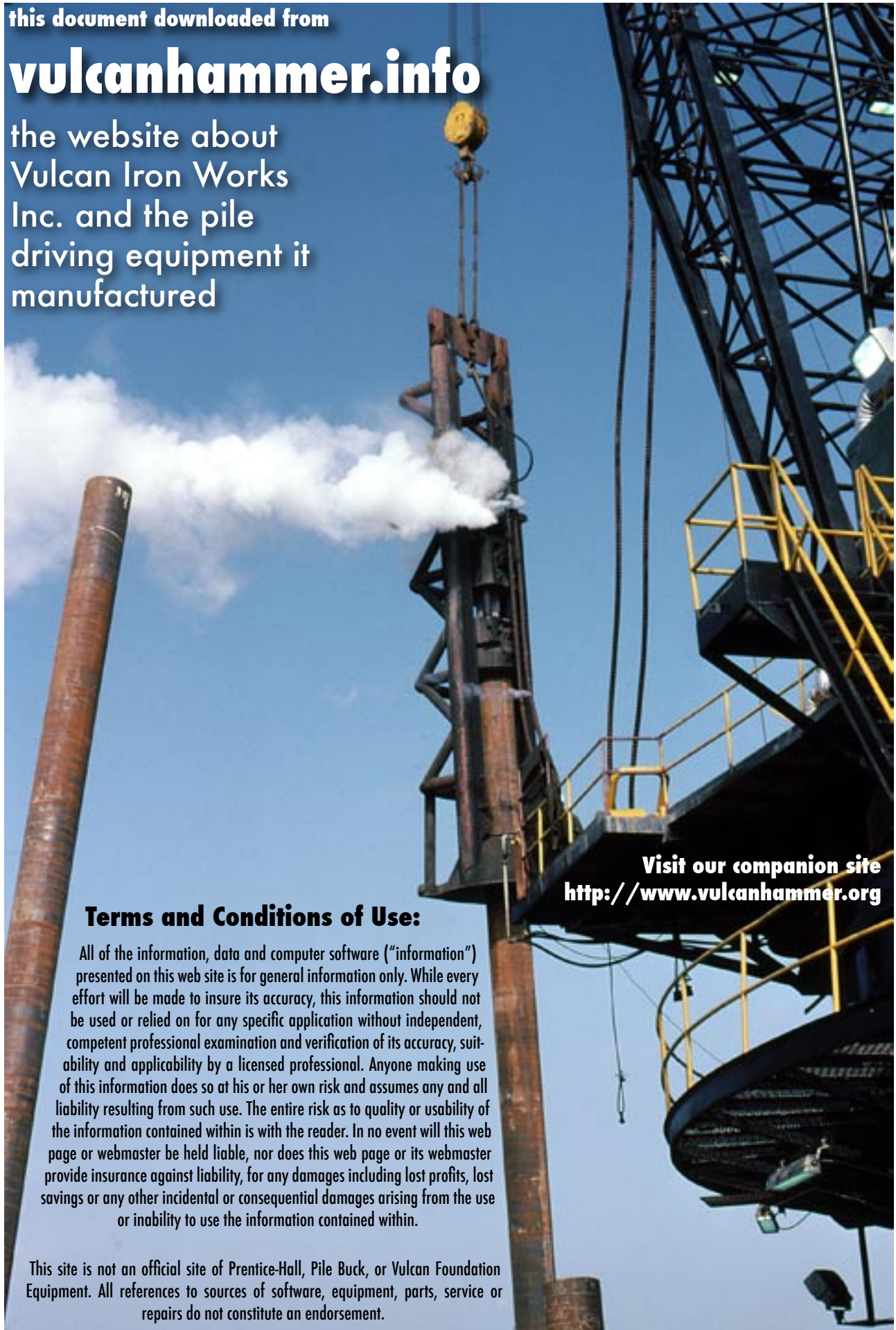
the website about  
Vulcan Iron Works  
Inc. and the pile  
driving equipment it  
manufactured

## Terms and Conditions of Use:

All of the information, data and computer software ("information") presented on this web site is for general information only. While every effort will be made to insure its accuracy, this information should not be used or relied on for any specific application without independent, competent professional examination and verification of its accuracy, suitability and applicability by a licensed professional. Anyone making use of this information does so at his or her own risk and assumes any and all liability resulting from such use. The entire risk as to quality or usability of the information contained within is with the reader. In no event will this web page or webmaster be held liable, nor does this web page or its webmaster provide insurance against liability, for any damages including lost profits, lost savings or any other incidental or consequential damages arising from the use or inability to use the information contained within.

This site is not an official site of Prentice-Hall, Pile Buck, or Vulcan Foundation Equipment. All references to sources of software, equipment, parts, service or repairs do not constitute an endorsement.

Visit our companion site  
<http://www.vulcanhammer.org>



EVALUATION OF PILE BEARING CAPACITY  
BY USE OF THE WAVE EQUATION

BY  
STUART H. WILLIAMS

---

A  
THESIS  
submitted to the faculty of the  
UNIVERSITY OF MISSOURI AT ROLLA  
in partial fulfillment of the requirements for the  
Degree of  
MASTER OF SCIENCE IN CIVIL ENGINEERING  
Rolla, Missouri  
1965

---

Approved by

Thomas S. Fry (advisor) John B. Stephens

James C. Maxwell

R. C. Hall

## ABSTRACT

The wave equation method of evaluating pile bearing capacity is investigated by using data obtained from a comprehensive pile testing program. Modifications which create a more accurate and realistic approach are made to the method proposed by previous investigators. With the use of these modifications, correlation between observed and computed results is more readily obtained.

Selected pile formulas in the empirical, static, and dynamic categories are reviewed so that a direct comparison between these and the wave equation method can be made.

## TABLE OF CONTENTS

	PAGE
ABSTRACT .....	ii
LIST OF ILLUSTRATIONS .....	iv
ACKNOWLEDGMENT .....	vi
I. INTRODUCTION .....	1
II. REVIEW OF LITERATURE .....	2
III. DISCUSSION .....	19
IV. CONCLUSIONS .....	47
BIBLIOGRAPHY .....	49
APPENDIX A .....	51
APPENDIX B .....	54
APPENDIX C .....	56
APPENDIX D .....	69
VITA .....	70

## LIST OF ILLUSTRATIONS

FIGURE		PAGE
1	Resistance Penetration Diagram .....	5
2	Portion of Elastic Rod .....	10
3	Free Body of Element $dx$ .....	10
4	Pile Mathematical Model Analogy .....	13
5	Boring Data .....	20
6	Driving Resistances of Test Piles .....	22
7	Load-Settlement and Load Distribution Curves .....	23
8	Resistance-Log Computed Set, Pile #1 .....	26
9	Resistance-Log Computed Set, Pile #2 .....	27
10	Resistance-Log Computed Set, Pile #6 .....	28
11	Resistance-Log Computed Set, Pile #1 .....	29
12	Resistance-Log Computed Set, Pile #2 .....	30
13	Resistance-Log Computed Set, Pile #6 .....	31
14	Resistance-Log Computed Set, Pile #1 .....	34
15	Resistance-Log Computed Set, Pile #2 .....	35
16	Resistance-Log Computed Set, Pile #6 .....	36
17	Resistance-Log Computed Set, Pile #1 .....	37
18	Resistance-Log Computed Set, Pile #2 .....	38
19	Resistance-Log Computed Set, Pile #6 .....	39
20	Resistance-Log Computed Set, Pile #1 .....	41
21	Resistance-Log Computed Set, Pile #2 .....	42
22	Resistance-Log Computed Set, Pile #6 .....	43
23	Resistance-Log Computed Set, Pile #1 .....	44

FIGURE		PAGE
24	Resistance-Log Computed Set, Pile #2 .....	45
25	Resistance-Log Computed Set, Pile #6 .....	46

## ACKNOWLEDGMENT

The author wishes to express his appreciation to Dr. Thomas S. Fry and John B. Heagler, Professors of Civil Engineering in the Civil Engineering Department of the University of Missouri at Rolla. Without their dedication to the advancement of knowledge concerning soils the author would not have been able to thoroughly appreciate all aspects involved in this investigation.

An expression of appreciation must also go to Herbert R. Alcorn of the Computer Science Center of the University of Missouri at Rolla for his unstinting assistance with programming and operation of the computer.

Above all, to my wife, whose patience and understanding throughout the course of this investigation was superb, I am deeply indebted.

## 1. INTRODUCTION

Throughout history, piles have been driven into the soil for the purpose of supporting various structures. With the great number of piles used for foundations, the development of an analytical method that would remove all doubt as to the actual bearing capacity of a pile would be a considerable contribution. Such a method would tremendously decrease the number of load tests required and the expense of overdesigning where load tests are not economically feasible.

Engineers, in their attempts to evaluate the bearing capacity of piles, have developed numerous mathematical formulas, 450 of which have been assembled by the Editors of the Engineering News Record. This large number of formulas clearly indicates a general lack of absolute reliability of any particular approach to give an accurate evaluation of pile bearing capacity when all field conditions are considered.

The goal, then, is to develop and prove reliable for all conditions a method that would give, consistently, an accurate estimation of the bearing capacity of a pile.

The purpose of this thesis is to present an analysis using the wave equation approach for the evaluation of the bearing capacity of a pile driven into cohesionless soil. The wave equation method will be compared with other more commonly used methods of pile bearing capacity determinations. In addition, the wave equation method as proposed and used by Smith (1) and Forehand and Reese (2) is evaluated and several alterations of their method, which account for size and shape of the pile and a more realistic soil reaction, are introduced.



## II. REVIEW OF LITERATURE

The many formulas developed to give the static bearing capacity of a pile can be grouped into empirical, static, dynamic, and wave equation methods of approach.

Empirical formulas, such as the one proposed by Gates (3) where

$$R = 48 \log \frac{10}{s} \quad (1)$$

where  $R$  = ultimate bearing capacity or resistance\* and

$s$  = penetration per blow for the last 6 inches,

are primarily based upon statistical data. This type of an approach may be quite adequate for a particular soil condition, hammer and pile, but universal application of empirical formulas has not been proven.

The static bearing capacity formulas are based on the assumption that total pile capacity is the sum of the pile point resistance plus the resistance due to side friction. This may be shown by

$$R = R_f + R_p \quad (2)$$

where  $R_f$  = fractional resistance along the sides of the pile and

$R_p$  = point resistance.

Krey (4) chose to show this relationship by

$$R = \frac{1}{2} \gamma U K_p + \gamma A_e L K_p \quad (3)$$

where  $\gamma$  = unit weight of the soil,

$\mu$  = coefficient of friction between the soil and pile,

\*Symbols once presented in an equation and explained will not be explained again unless a distinct meaning is intended. Appendix A contains a list of all symbols used.

$U$  = perimeter of the pile,

$K_p$  = coefficient of passive earth pressure,

$A_e$  = effective cross-sectional area of the pile

$L$  = length of the pile.

This approach assumes that the side frictional resistance is uniform along the length of the pile and that the full passive earth pressure is developed. The impossibility of properly evaluating side friction and the coefficient of earth pressure along the total length of the pile, at the failure load, makes this approach unreliable.

The largest number of pile formulas in existence are in the dynamic category. A more thorough development of the dynamic approach is presented in order to point out the errors which result from the various simplifying assumptions that are made. This is done so that a comparison with the wave equation method can be made.

The basic reasoning underlying dynamic pile formulas is to derive the resistance,  $R$ , from energy relationships developed by the last blows of the hammer. Fundamentally this can be shown by

$$Wh = R_s, \text{ which gives} \quad (4)$$

$$R = \frac{Wh}{s} \quad (5)$$

where  $W$  = weight of the hammer and

$h$  = height of fall of the hammer.

The simplicity of the relationships indicated in equation (4) is nullified by the  $R_s$  portion of the equation. Complications arise from the fact that the dynamic resistance to driving is not a reliable measure of the final static resistance and is not a constant during the

penetration of the pile. Other sources of errors included in this portion of the equation are that the distances includes elastic compressions of the pile and soil along with the plastic or permanent penetration of the pile into the soil, and that loss of energy due to impact is not accounted for.

The probable resistance - penetration relationship for one blow of the hammer on a pile driven into a cohesionless soil has been presented by Cummings (5). In Figure 1 the resistance to penetration is plotted on the abscissa and the penetration plotted on the ordinate. The right hand portion of equation (4) is represented by the area ORBS which indicates that the resistance to penetration is constant throughout the penetration. However, it is more reasonable to expect that the resistance-penetration relationship would be more accurately indicated by area OAS, where resistance varies with penetration. The maximum or dynamic resistance to penetration then becomes  $R'$ . The area OAS' represents the total energy dissipated following one hammer blow and the area SAS' is the energy absorbed by the elastic compression of the pile and soil. These elastic compressions are represented by SS'.

The energy relationships then can be shown as

$$W_h = CRs + E_1 \quad (6)$$

where  $CRs$  = area OAS from Figure 1,

$C$  = a coefficient to increase soil resistance due to dynamic penetration

$E_1$  = energy losses due to elastic compression of the pile and soil.

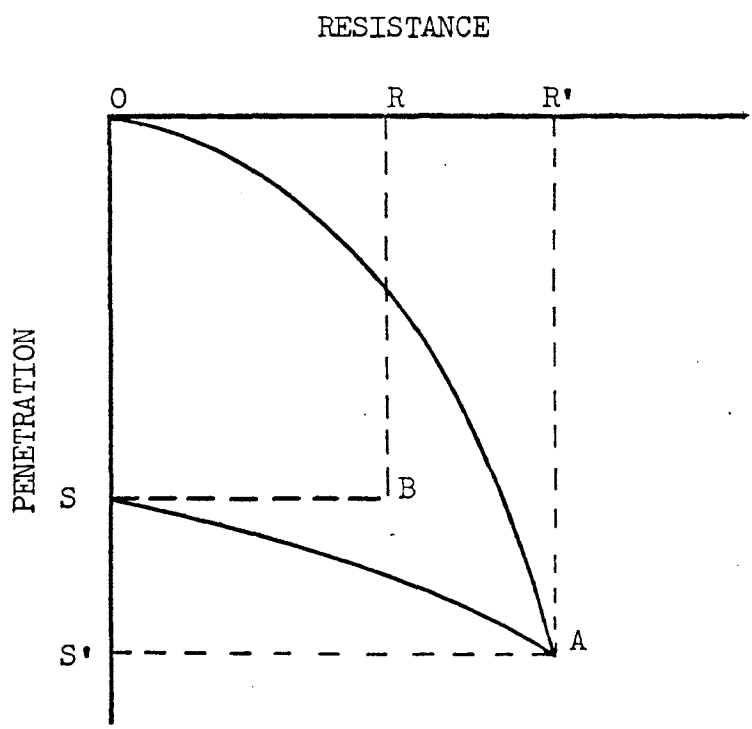


FIGURE 1. RESISTANCE-PENETRATION DIAGRAM  
After Cummings (5)

Energy losses due to impact are still unaccounted for, but equation (6) may be altered to include these by adding a term  $K_i$  representing impact losses so that

$$Wh = CRs + E_1 + K_i \quad (7)$$

It is the  $K_i$  and  $E_1$  terms of equation (7) and the assumptions as to how they should be handled mathematically that has led to the large number of dynamic pile formulas, and consequently their inability to give consistent results. In addition all formulas ignore the C coefficient thereby treating R as a constant. Hammer efficiency can be included by multiplying the Wh term by an efficiency factor suitable for the pile driving equipment being used. However hammer efficiency will not be included in the following discussion.

If the C coefficient and the  $K_i$  term are ignored and only that energy involved in the elastic compression of the pile is accounted for in the  $E_1$  term then

$$Wh = Rs + \frac{R^2 L}{2AE} \quad (8)$$

which gives

$$R = - \frac{sAE}{L} + \left[ \frac{2WhAE}{L} + \left( \frac{sAE}{L} \right)^2 \right]^{\frac{1}{2}} \quad (9)$$

where A = cross sectional area of the pile material,

E = modulus of elasticity of the pile material.

Equation (9) was developed by Weisbach about 1850. This equation is inadequate because no allowance is made for the dynamic change in soil resistance, the compression is in terms of static terms when in fact it should be in dynamic terms, and all the resistance to penetration is assumed to act at the pile point.

Using Newtonian theory developed for two free massive bodies to find energy losses due to impact, Cummings (5) states that

$$K = \frac{WhP(1-e^2)}{W+P} \quad (10)$$

where  $P$  = weight of pile and

$e$  = coefficient of restitution.

When equation (10) is substituted in equation (7) for the  $K_1$  term and the  $C$  and  $E_1$  terms ignored then

$$Wh = Rs + \frac{WhP(1-e^2)}{W+P} \quad (11)$$

which gives

$$R = \frac{Wh}{s} \left( \frac{W+Pe^2}{W+P} \right) \quad (12)$$

If  $e$  is assumed to be zero, inelastic impact, equation (12) reduces to

$$R = \frac{Wh}{s \left( 1 + \frac{P}{W} \right)} \quad (13)$$

Equation (13) was published by Eytelwein about 1820.

If  $e$  is taken as 1.0, perfectly elastic impact, equation (12) reduces to

$$R = \frac{Wh}{s} \quad (14)$$

which is identical to equation (5).

If in equation (12), a factor of safety of 6 is used, a factor  $k$  is added to  $s$  to allow for elastic compressions, and the weight of the pile is ignored then

$$R = \frac{2Wh}{(s+k)} \quad (15)$$

which is the Engineering News Formula developed by Wellington in 1858.

Equations (13), (14) and (15) do not account for dynamic changes in soil resistance and through their various assumptions fail to account accurately for energy losses due to impact.

When all energies are accounted for as proposed by Redtenbacher about 1859 then

$$Wh = R_s + \frac{WhP(1-s^2)}{W+P} + \frac{R^2 L^2}{2A^2 E^2} + \frac{R^2 L}{2AE} + \frac{QR}{2} \quad (16)$$

where  $L^2$  = length of the pile cap,

$A^2$  = cross-sectional area of the pile cap,

$E^2$  = modulus of elasticity of the pile cap material, and

$Q$  = amount of elastic compression of the soil.

If equation (16) is altered so that

$C_1 = \frac{RL^2}{A^2 E^2}$  = assumed elastic compression of the pile cap, and

$C_2 = \frac{RL}{AE}$  = assumed elastic compression of the pile, then

$$Wh = R_s + \frac{WhP(1-s^2)}{W+P} + \frac{C_1 R}{2} + \frac{C_2 R}{2} + \frac{QR}{2} \quad (17)$$

and

$$R = \frac{Wh}{\left[ s + \frac{1}{2} (C_1 + C_2 + Q) \right] \left( \frac{W + Pe^2}{W + P} \right)} \quad (18)$$

which is the Hiley Formula.

It is quite apparent at this point that numerous assumptions can be made and that for each assumption or combination of assumptions a dynamic formula for the bearing capacity of a pile can be developed. Many formulas, other than those presented here can be found in literature on pile driving.

The existing empirical, static, and dynamic formulas do not properly evaluate the complete pile driving equipment-pile-soil

system. Proper evaluation requires that pile size, shape, and elastic properties along with the elastic and plastic properties of the soil be correctly considered. The wave equation approach to the evaluation of pile bearing capacity takes into consideration, in a more accurate manner, all the parameters that are involved.

In the wave equation approach the pile is treated as an elastic rod which is struck on one end. When the elastic rod shown in Figure 2 is struck at one end a strain wave will be set up which travels along the rod. A section at a distance  $x$  from the left end of the rod will be displaced a distance  $u$ . A section at a distance  $x + dx$  will be displaced a distance  $u + du$ . Since the element  $dx$  is displaced a distance  $du$  then the unit strain can be represented as  $\frac{\partial u}{\partial x}$ . The partial derivative is used because the displacement  $u$  is a function of both time,  $t$ , and distance  $x$ .

The stress on the section at  $x$  is then

$$\sigma = E \frac{\partial u}{\partial x} \quad (19)$$

and the force on section  $x$  is

$$F = EA \frac{\partial u}{\partial x} \quad (20)$$

From the forces acting on the element  $dx$ , shown in Figure 3, the motion of the element can be described by

$$F = MA, \text{ or} \\ -EA \frac{\partial u}{\partial x} + EA \left( \frac{\partial u}{\partial x} + \frac{\partial^2 u}{\partial x^2} dx \right) = (\rho A dx) \frac{\partial^2 u}{\partial t^2} \quad (21)$$

which gives

$$\frac{\partial^2 u}{\partial t^2} = \frac{E}{\rho} \frac{\partial^2 u}{\partial x^2} \quad (22)$$



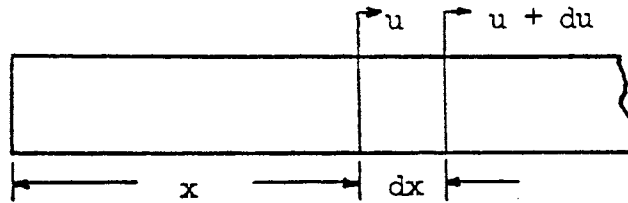
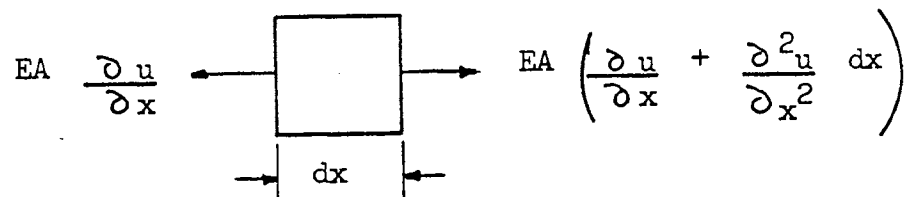


FIGURE 2. PORTION OF ELASTIC ROD

FIGURE 3. FREE BODY OF ELEMENT  $dx$

where  $\rho$  = mass per unit volume.

Equation (22) is a form of the wave equation. For use in pile driving analysis a term representing soil resistance along the side of the pile and at the pile point is added so that

$$\frac{\partial^2 u}{\partial t^2} = \frac{E}{\rho} \frac{\partial^2 u}{\partial x^2} + R \quad (23)$$

Boussinesq (5) solved equation (23) for the maximum stress at the fixed end of the rod when the ratio of  $W/P$  is less than 5 and found

$$\sigma_{\max} = \frac{2EV}{a} \left( 1 + e^{-\frac{2P}{W}} \right) \quad (24)$$

where  $\sigma_{\max}$  = maximum stress at fixed end,

$V$  = velocity of the striking hammer,

$a$  = velocity of stress wave in the rod, and

$e$  = base of the natural logarithm.

The same assumptions that are incorporated in equation (23) also govern equation (24) and as stated by Cummings (5) are listed as follows:

1. that the sides of the pile are free and that there is no side friction which would affect the stress waves traveling up and down the pile,
2. that stress waves in the hammer may be neglected,
3. that there are no flexural vibrations of the pile,
4. that the pile behaves as a linearly elastic rod,
5. that the hammer strikes directly on the head of the pile and that the surfaces of contact are two ideal smooth parallel planes, and
6. that the lower end of the pile is fixed.

Smith (6) developed equations, which are equivalent to the difference solution of equation (23), describing the forces and motions created following the impact of the ram on the pile. These equations were derived from an analogous mathematical model consisting of weights, springs and resistances, representing the ram-pile-soil system. The pile and mathematical model are shown in Figure 4.

Smith's fundamental equations are as follows:

$$D_m = d_m + v_m (12dt), \quad (25)$$

$$C_m = D_m - D_{m-1}, \quad (26)$$

$$F_m = C_m K_m, \quad (27)$$

$$\Sigma_m = F_{m-1} - F_m - R_m, \text{ and} \quad (28)$$

$$V_m = v_m + \Sigma_m \frac{dt}{W_m}, \quad (29)$$

where the following apply to the time interval n:

$D_m$  = displacement of weight m in time interval n,

$C_m$  = compression of spring m in time interval n,

$F_m$  = force exerted by spring m in time interval n,

$K_m$  = spring constant for spring m,

$R_m$  = resistance applicable to weight m in time interval n,

$V_m$  = velocity of weight m in time interval n,

$W_m$  = weight of weight m,

$\Sigma_m$  = net accelerating force acting on weight m in the time

interval n,

and the corresponding small letters refer to the previous time interval

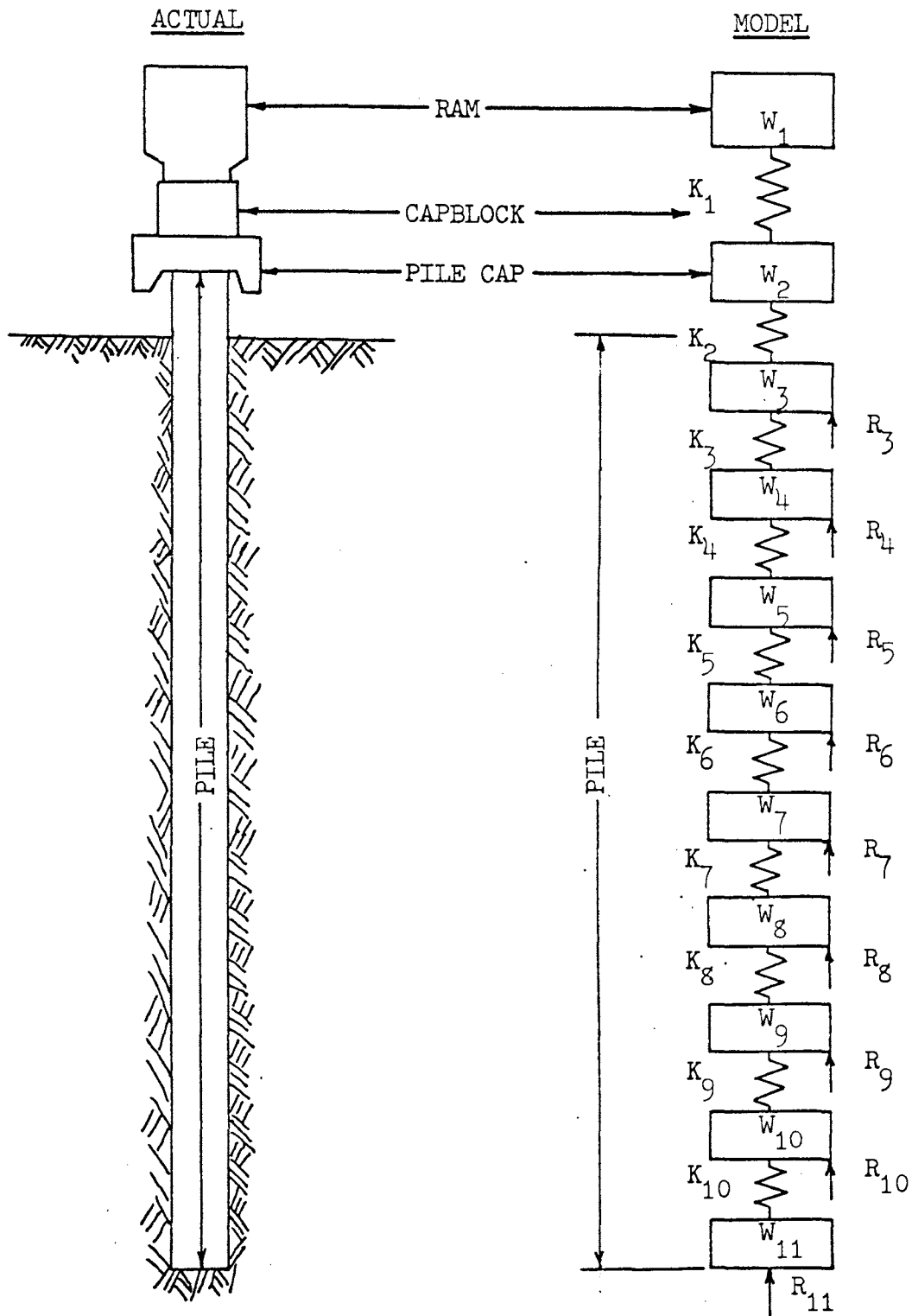


FIGURE 4. PILE MATHEMATICAL MODEL ANALOGY  
After Smith (1)

n-1. The term  $dt$  is the time interval, which for steel is normally taken as  $1/4000$  sec.

Smith (1) developed a method of mathematical analysis which is best solved by an electronic computer, by:

1. combining equations (28) and (29) to eliminate the necessity of calculating  $Z_{\frac{1}{2}}$ ,
2. introducing restitution in the pile cap and cushion block to account for energy losses in these two elements,
3. applying a viscous damping constant so that resistance to penetration will vary with the velocity of penetration, and
4. using an idealized stress strain relationship for the soil, with  $\epsilon_0$  as the maximum elastic strain.

Through the use of this method the bearing capacity of a pile can be very accurately evaluated.

When this method is applied for one blow of the hammer the incremental and total displacements, compressions, forces, and velocities, during successive time intervals,  $dt$ , are calculated for each weight or spring of the mathematical model. The calculations are stopped when one of four conditions occurs. These conditions are as follows:

1. when the velocity of the pile cap exceeds twice the ram velocity, this condition exists when the pile plunges into the soil;
2. when the velocity of the pile tip exceeds twice the ram velocity, this condition exists when the pile plunges into the soil;
3. when penetration by the pile point ceases, and
4. when all velocities become simultaneously negative or zero, which also indicates that penetration has ceased.

As to the assumptions governing the wave equation, Smith states that all but 3 and 5 are allowed for by his method. Cummings (5) indicates that assumption 3 is considered to be highly unlikely and good pile driving practice will meet the requirements of assumption 5.

To use Smith's method, for each combination of pile driving equipment, pile, and soil, the following assumptions must be made:

1. the amount of elastic compression of the soil, this factor, previously indicated as  $Q$ , is used to determine the soil spring constant by

$$K'_m = \frac{R}{Q} \quad (30)$$

where  $K'_m$  = spring constant for the soil resisting movement of weight  $m$ . Once the amount of penetration reaches a value of  $Q$ , plastic penetration takes place;

2. the value of the coefficient of viscous damping for the soil, this value is used to determine the increase in soil resistance due to dynamic penetration by

$$R_d = R_s (1 + JV'_m) \quad (31)$$

where  $R_d$  = dynamic resistance,

$R_s$  = static resistance, and

$J$  = viscous damping coefficient of the soil resisting penetration of the pile point and  $J' = J/3$  is the viscous damping coefficient of the soil along the side of the pile;

3. the distribution of resistance between side friction and point resistance,

4. the distribution of side friction or resistance along the length of the pile;

5. the ultimate resistance or bearing capacity of the pile.

Appendix B lists the information required to accurately utilize Smith's equations to obtain reliable results.

Assumptions 1 and 2 are used in determining the resistance to penetration by

$$R_p = (D_p - D_p^e) K_p^e (1 + Jv_p), \text{ and} \quad (32)$$

$$R_m = (D_m - D_m^e) K_m^e (1 + J^e v_m) \quad (33)$$

where  $R_p$  = point resistance to driving,

$D_p$  = displacement of the pile point in time interval  $n$ ,

$D_p^e$  = plastic displacement of soil beneath the pile point in

time interval  $n$ ,

$K_p^e$  = soil spring constant beneath the pile point,

$K_m^e$  = soil spring constant for the side of pile,

$D_m^e$  = plastic deformation of soil at weight  $m$  in time interval  $n$ ,

$v_p$  = velocity of the pile point in the previous time interval  $n-1$ ,

and

$v_m$  = velocity of weight  $m$  in the previous time interval  $n-1$ .

Forhand and Reese (2) elaborated on the computer program presented by Smith and presented the complete program in Fortran language. They also show that equations (25) through (29) are equivalent to the difference solution of the wave equation.

By using data from a number of piles for which driving and test data were available, they varied the values for which assumptions must be made. For each value assumed for  $Q$ ,  $J$ ,  $J'$ , when values for assumptions 3, 4, and 5 were known from pile tests, they were able to obtain a range of values for  $Q$ ,  $J$ , and  $J'$ . These values for cohesionless soil are,

$$\begin{aligned} Q & .1 - .2 \text{ in.} \\ J & .15 - .2 \\ J' & .05 - .067 \end{aligned}$$

The lower values also correspond to those proposed by Smith (1).

Seed and Lundgren (7) in studying strength characteristics of saturated sands with a void ratio,  $e$ , of .585, under rapid rates of loading found that the strength of the rapidly loaded undrained sand under a lateral confining pressure of 2 Kg/cm<sup>2</sup> was about 40% greater than the same sand under a static drained test. The strength gain is attributed to both dilatancy effects and the high rate of loading. Sands with greater void ratios were tested in a similar manner and strength gain decreased to 0% for a sand with  $e = .78$ .

In a study of the shear strength of rapidly loaded undrained saturated sands, as determined by triaxial testing procedures, Whitman and Healy (8) found that the friction angle increases about 10% as time to failure is decreased. But, because of experimental difficulties they feel that in actuality the angle change is less than 1°. They also found that dense ( $e = .50$ ) saturated sands exhibited no other increase in strength with increased strain rate whereas loose ( $e = .65$ ) sands gave a 40% increase in strength with an increase in strain rate. This



difference is attributed to the relative time - dependency of the excess pore water pressure.

Selig and McKee (9) in tests involving both static and dynamic loading of small footings on dry sand found that settlements under dynamic loads increase linearly with the energy of impact for each size of footing tested. Also settlement became larger at an increasingly greater rate for progressively smaller footings under the same impact energy.

From the data presented by Selig and McKee it is found that the ratio of the dynamic bearing capacity to the static bearing capacity varies linearly with footing width, increasing with increasing footing width.

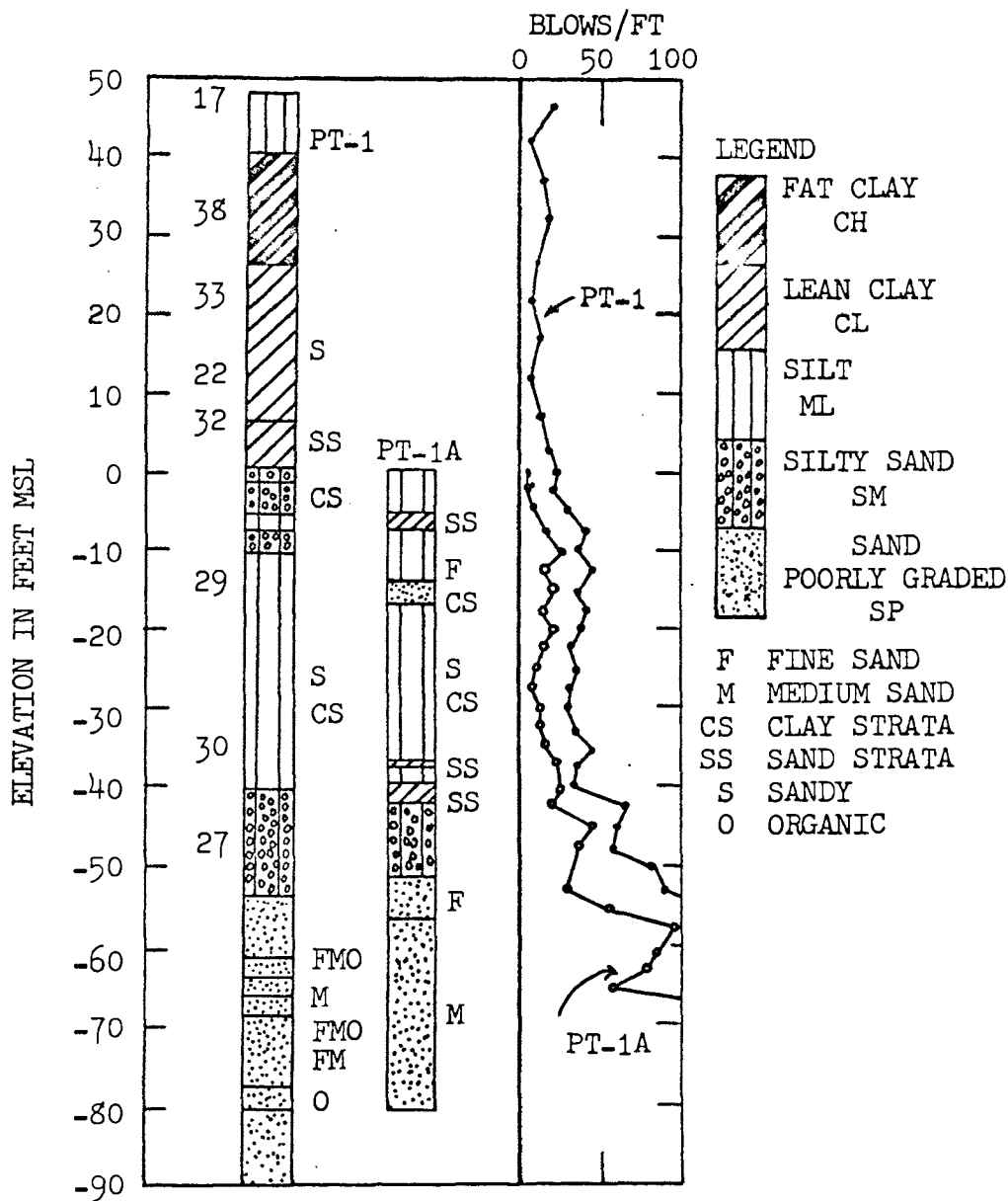
## III. DISCUSSION

The wave equation approach to the evaluation of the pile bearing capacity accounts for all the factors involved in the dynamic driving - static loading relationship. However, when the dynamic system present during the driving of the pile is resisted by soil with its own peculiar dynamic and static properties, a reliable solution becomes dependent upon the proper evaluation of these properties. Pile bearing capacity then, as evaluated by the wave equation, becomes a function of the static and dynamic properties of the soil.

This study is based upon information obtained from pile tests conducted by the U. S. Army, Corps of Engineers and reported by Mansur and Kaufman (10).

The piles were driven from the bottom of an excavation created by the removal of 50 feet of overburden. Soil conditions at the test site are represented by the bearing data shown in Figure (5). Soils beneath the bottom of the excavation consist of alternating strata of silts and silty sands, with interspersed clay strata, for a total thickness of 50 to 60 feet. Clean sands with a thickness of 40 to 60 feet lie beneath the silty soils and on top of an unspecified thickness of stiff tertiary clays.

Laboratory tests on undisturbed samples of the silts and sandy silts gave an internal angle of friction,  $\phi$ , of  $28^{\circ}$  and cohesion of 0.1 ton per square foot. These values were determined by consolidated - undrained triaxial tests and consolidated - drained direct shear tests.



NOTE: Driving resistances (blows per foot) determined with a standard split spoon sampler (1-3/8 in. ID. 2-in OD) and a 140-lb. hammer dropped 30 inches. Boring advanced with fishtail using drilling mud. Figures to left of Borings are natural water contents in percent dry weight. Boring PT-1 made from ground surface in August 1954. Boring PT-1A made from bottom of excavation (elev 0) in February 1955. Boring classified in accordance with the unified soil classification system used by the Corps of Engineers, U. S. Army.

FIGURE 5. BORING DATA  
After Mansur and Kaufman (10)

An average value of  $\phi = 36^\circ$  for the sands was determined from consolidated - drained triaxial tests on both undisturbed and remolded samples.

A Vulcan No. OR ram was used to drive all the piles. The ram weighed 9300 pounds, had a stroke of 39 inches and developed 30,200 foot pounds of energy. Velocity at the instant prior to impact, as determined by

$$V = \left( \frac{\text{Rated Energy} \times \text{efficiency} \times 64.4}{\text{weight}} \right)^{\frac{1}{2}} \quad (34)$$

was 12.6 ft/sec when a hammer efficiency of .75 (10) is assumed.

Driving resistances of the three test piles are shown in Figure (6).

All test piles were instrumented with strain gauges which allowed determination of load distribution along the pile and the ratio of point bearing to total bearing capacity of the pile. Load-settlement and load distribution curves for the test piles are shown in Figure (7).

The computer program listed in Appendix (C), which is the program presented by Forehand and Reese, with minor changes so that it could be used on an IBM 1620 Model II computer, was used with the pile driving and test data reported by Mansur and Kaufman.

The distribution of the side friction along the piles was taken from Figure (7) as being rectangular with each incremental length of pile providing the same amount of resistance. The values of  $Q$ ,  $J$  and  $J'$  were taken as .1, .15, and .05 respectively.

For each value of total resistance assumed, the penetration resulting from one blow is computed. The reciprocal of the penetration following this one blow is defined as set.

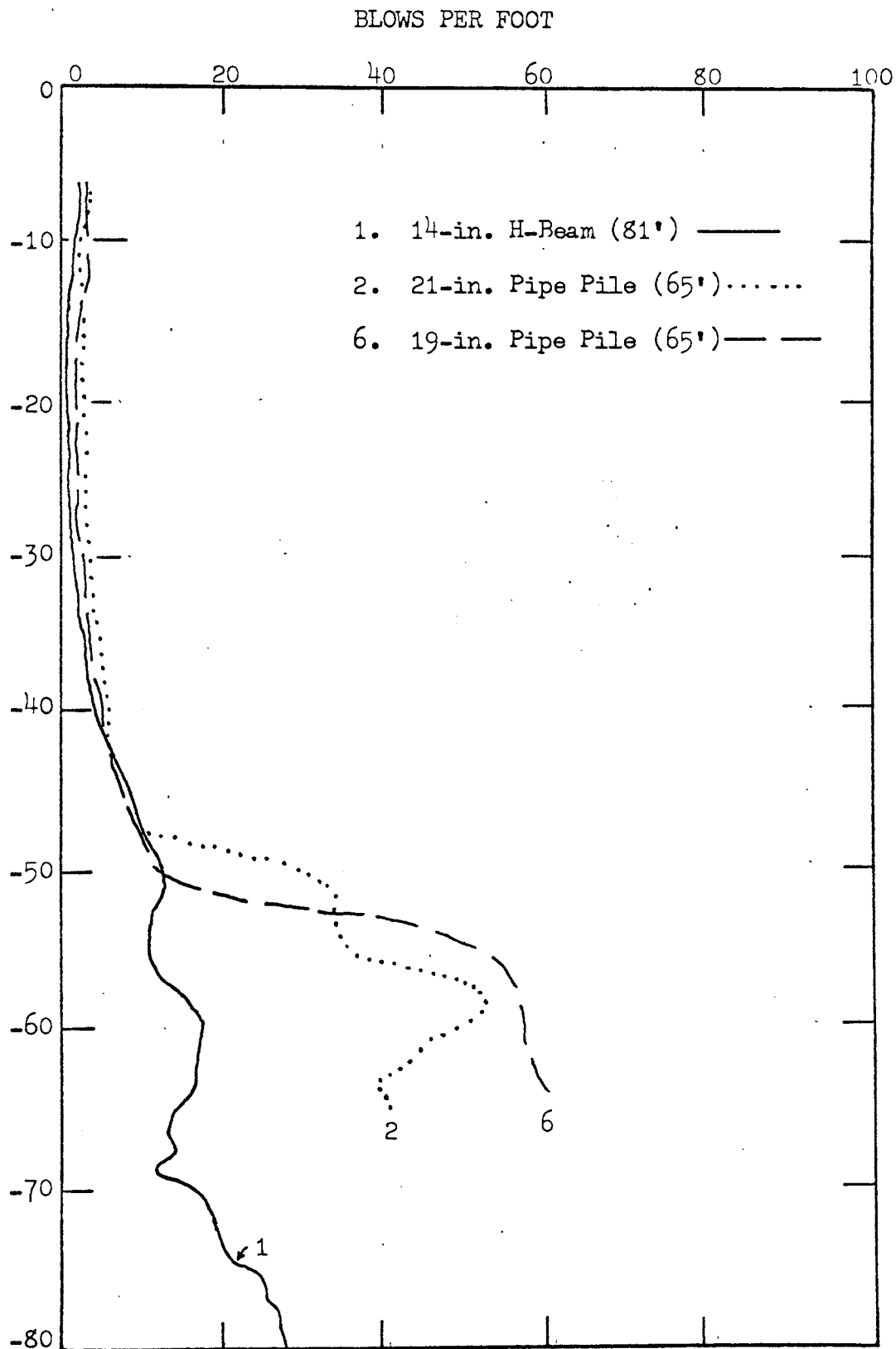


FIGURE 6. DRIVING RESISTANCES OF TEST PILES  
After Mansur and Kaufman (10)

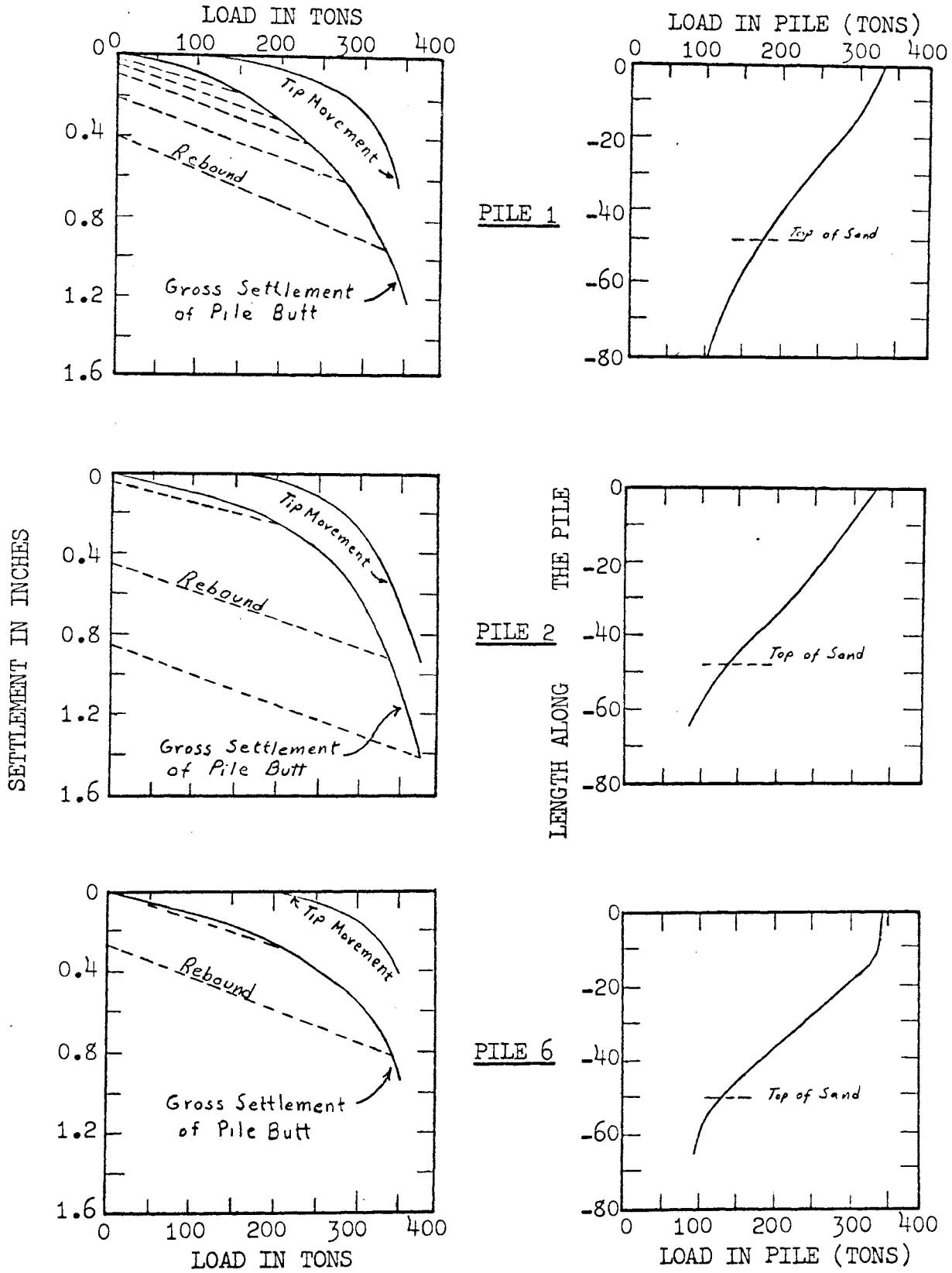


FIGURE 7. LOAD-SETTLEMENT AND LOAD DISTRIBUTION CURVES  
After Mansur and Kaufman (10)

<u>File</u>	<u>Size Type and Length</u>	<u>Final Elows/in</u>	<u>Total Fail Load (Tons)</u>	<u>% Point R Total Load</u>	<u>Failure Load in Sand/Tons</u>	<u>Penet in Sand (Ft)</u>	<u>% Point R Sand Only</u>
1	14 in H-Beam 81 ft long	2.66	296	34	142	32	68
2	**21 in pipe pile 3/8 in wall thick 65 ft long	3.33	300	28	110	17	66
6	**19 in pipe pile 3/8 in wall thick 65 ft long	5.33	342	29	127	15	65

\*\*Effective diameter due to strain gauge installation, actual OD is 1 inch less

TABLE I. PILE DATA

The computed resistance - set relationship for the piles, following Smith's procedure, are shown in Figures (8) through (13). Each curve represents a different distribution of resistance between point bearing and side friction. These distributions are as follows:

- A - 100% point, 0% side
- B - 75% point, 25% side
- C - 50% point, 50% side
- D - 25% point, 75% side
- E - 0% point, 100% side

Two groups of curves are shown for each pile. One is for "no load = 2" which indicates that the movement of all but the top 2 weights, of the mathematical model (Figure 4), is being resisted by the soil. The other is when "no load = 8, 9 or 12," depending on the particular pile, which indicates that the movement of only those weights in the sand layer is being resisted. This is the actual driving case. A comprehensive explanation of the interpretation of Figures 8 through 25 is contained in Appendix D.

If the evaluation by the wave equation is correct then the final computed set or driving resistance should correspond with the static load test failure load in the sand layer. In Figure (8), close correlation between observed and computed set is obtained for the H-pile in the sand layer, but in Figures (9) and (10) no correlation can be obtained for the pipe piles in the sand layer.

The resistance to driving by the silty layers can be considered negligible after a few blows of the hammer, due to changes in relative density and pore pressures under dynamic loading. However Yang (12) presents evidence that resistance will be increased by a factor of



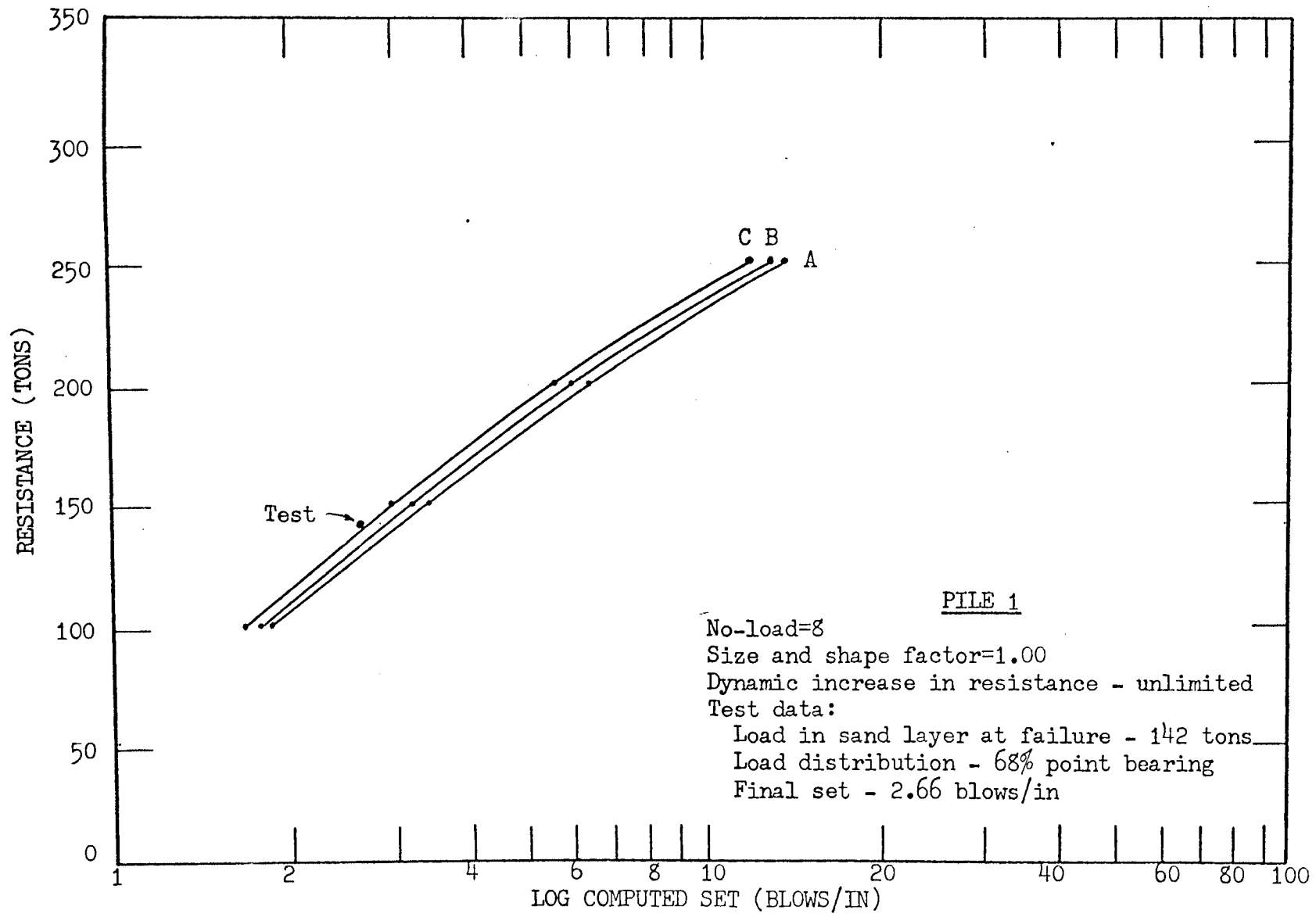


FIGURE 8. RESISTANCE - LOG COMPUTED SET

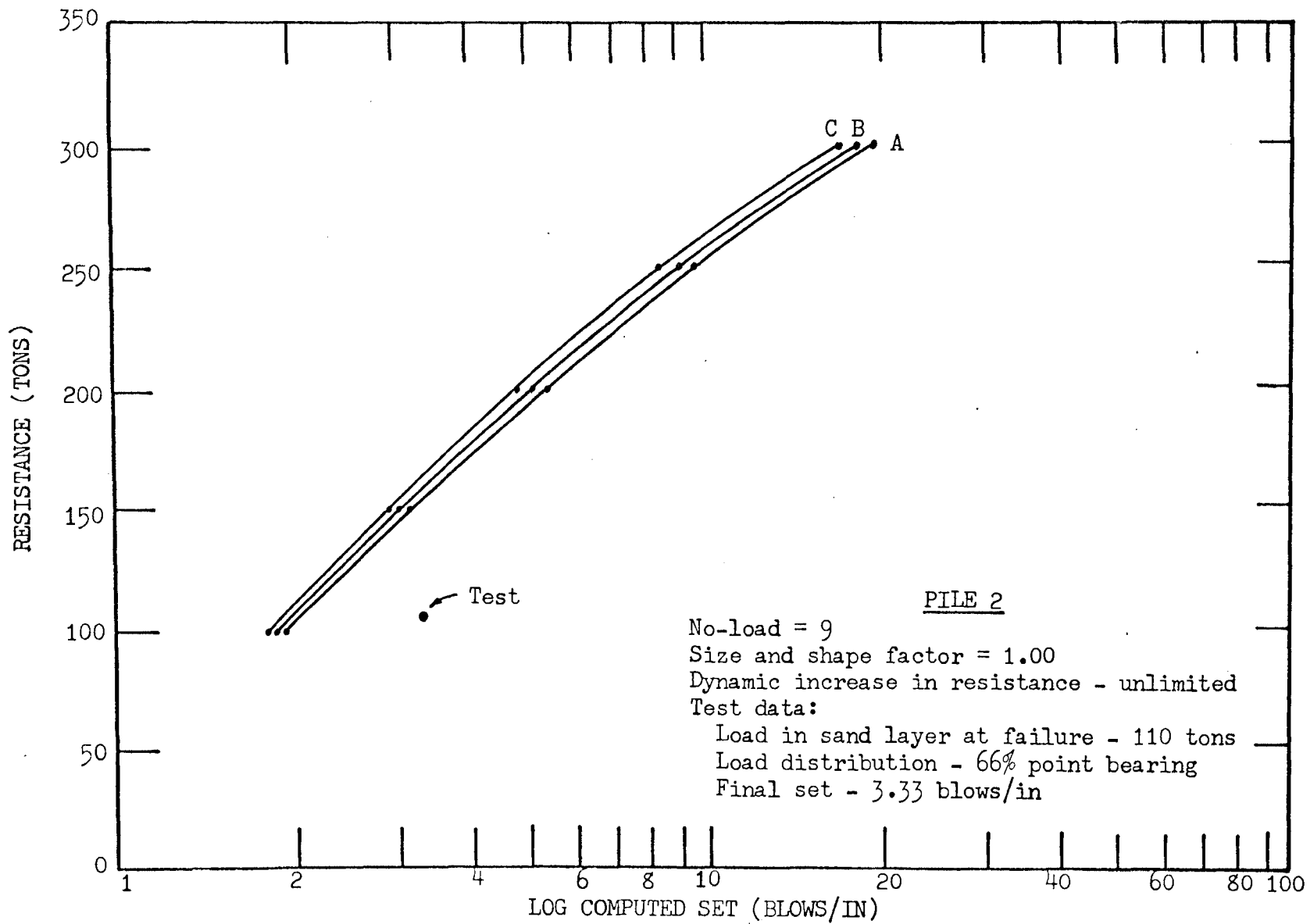


FIGURE 9. RESISTANCE - LOG COMPUTED SET

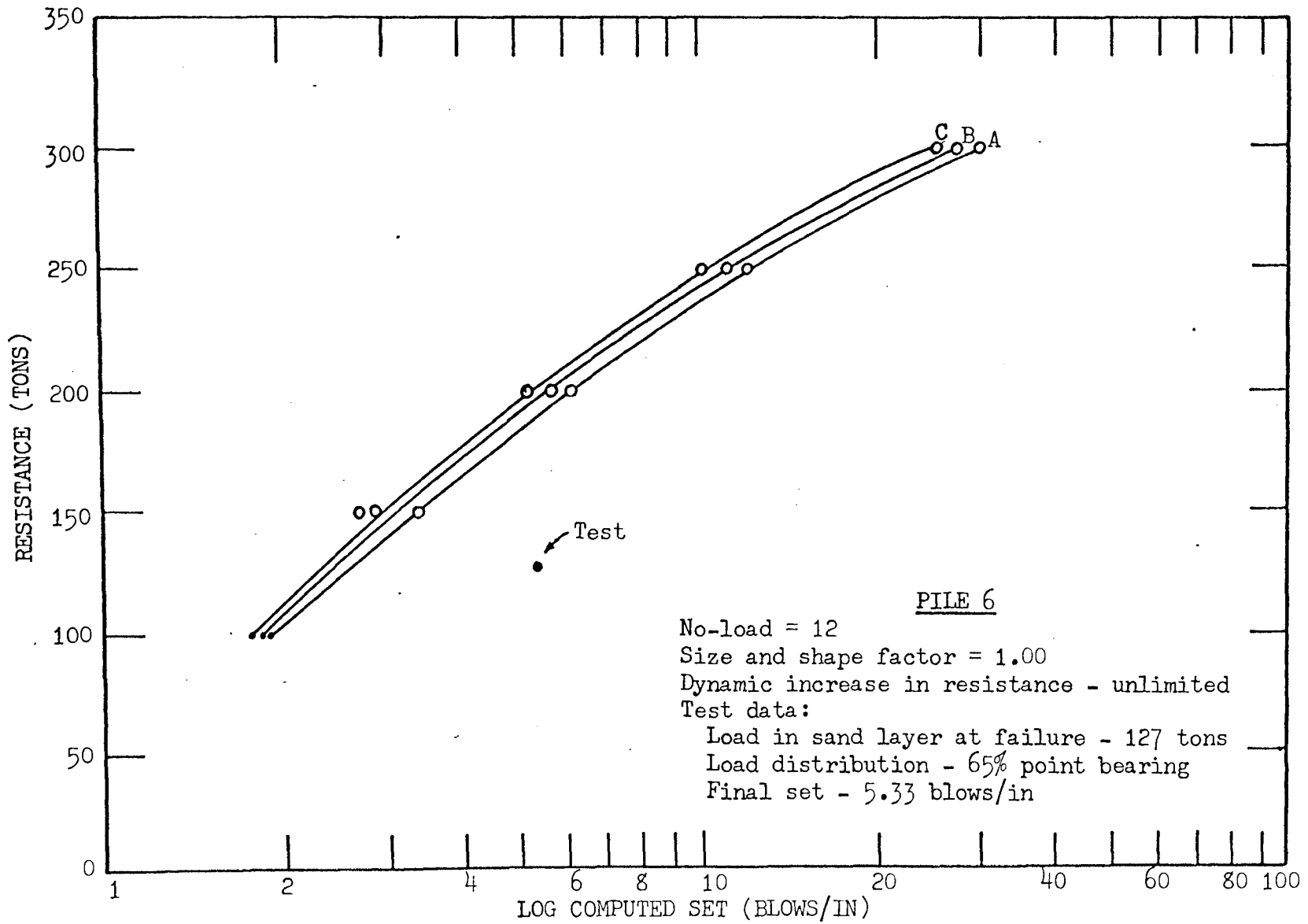


FIGURE 10. RESISTANCE - LOG COMPUTED SET

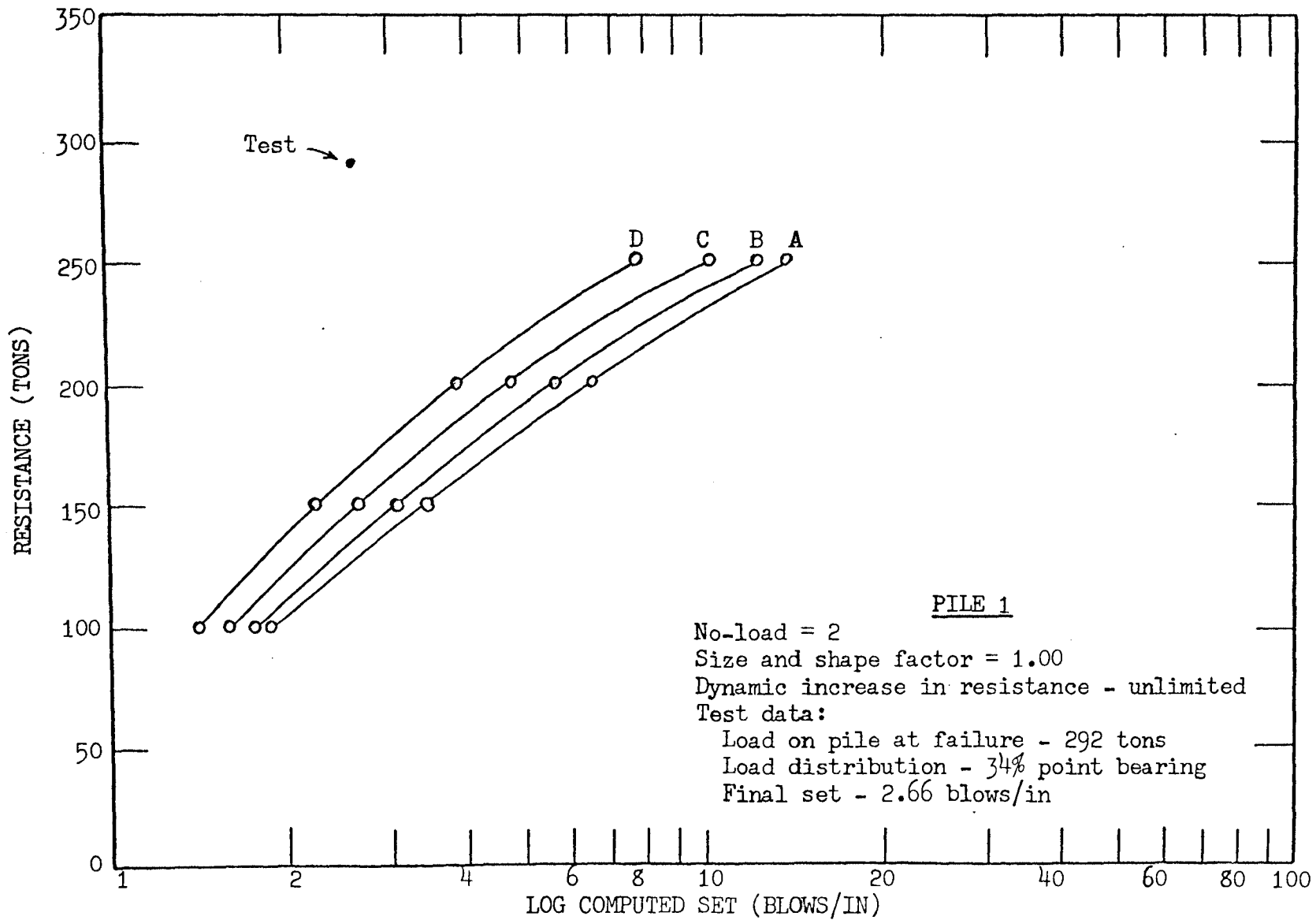


FIGURE 11. RESISTANCE - LOG COMPUTED SET

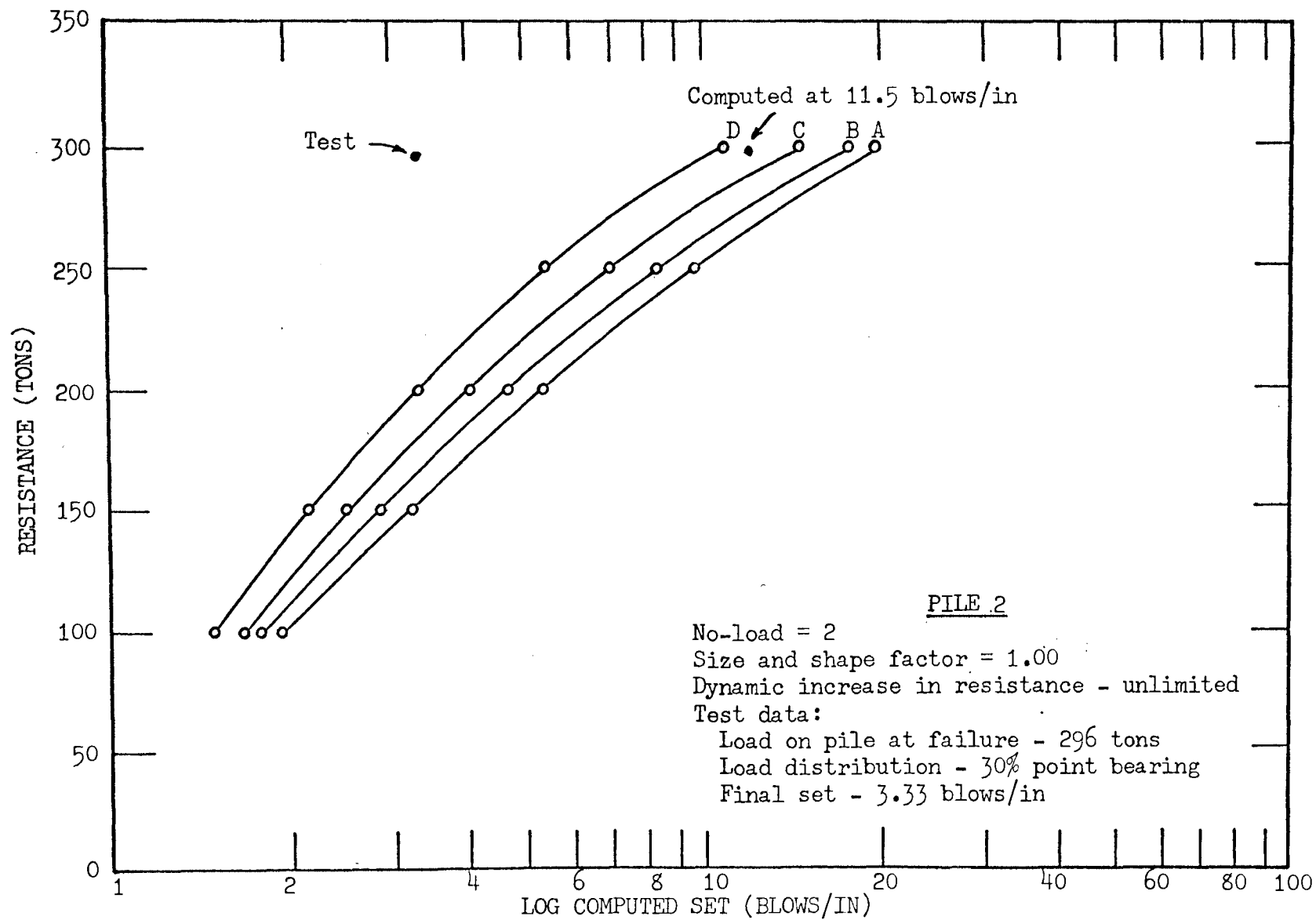


FIGURE 12. RESISTANCE - LOG COMPUTED SET

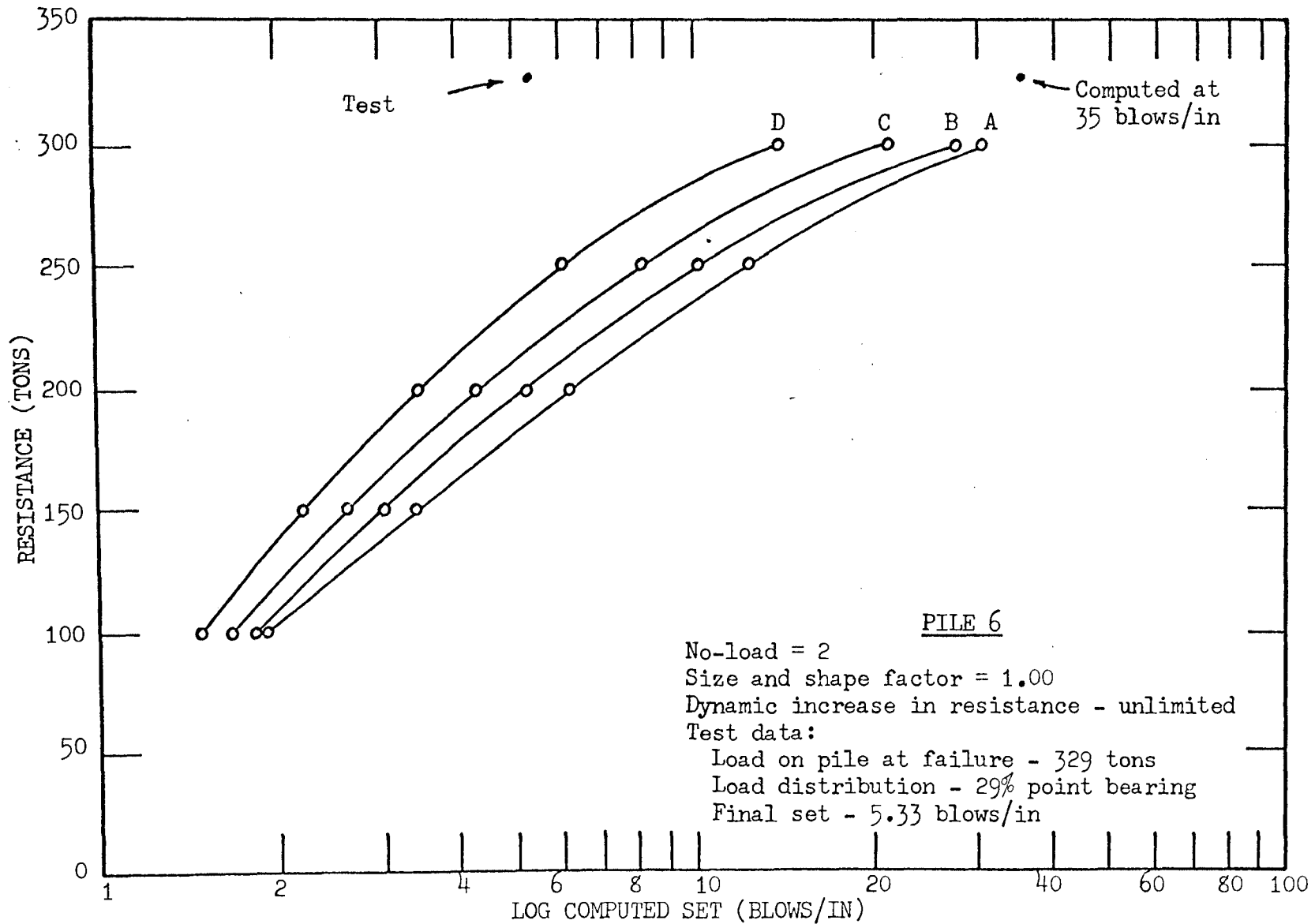


FIGURE 13. RESISTANCE - LOG COMPUTED SET

10 to 12 some time after driving has ceased and the system has come to equilibrium. Moreover, the driving resistance by dense sands will be greater than their static resistance because of relative density and pore pressure changes. Yang also predicts that the equilibrium resistance of piles driven into dense sand will be approximately  $1/2$  the resistance to driving after a number of blows.

The final resistance to driving for each pile is developed almost entirely in the sand layer so that the final computed set for the total pile should be 5 to 6 times the final driving resistance. By applying this reasoning when the soil provides resistance to penetration of the total pile (Figures 11, 12 and 13) correlation between observed and computed relationships can only be obtained for pile 6.

Neither Smith nor Ferehand and Reese take into account the size of the pile in their computations determining the resistance offered by the soil. From equation (24) it can be seen that the maximum stress in a pile is not related to the shape of the pile. If an H and pipe pile have identical cross sectional area of steel, the maximum stress at the point will be the same. However, the area of soil providing resistance is different due to the non-identical shapes and effective penetrating areas of the two piles. Therefore the resistance to penetration for each type of pile will be different and the size and shape of the pile should be considered. This is also indicated by the work of Selig and McKee in connection with the dynamic loading of small footings and the driving resistance curves of Figure (6).

In order to provide for variations in pile sizes and shapes, equations (32) and (33) have been modified so that

$$R_p = (D_p - D_p^*) K_p (1 + Jv_p) AF, \text{ and} \quad (35)$$

$$R_m = (D_m - D_m^*) K_m (1 + J^*v_m) AF \quad (36)$$

The AF term of equations (35) and (36) is used to increase soil resistance according to some function of the effective area, and shape of the pile.

A searching procedure was used on the IBM 1620 II computer to determine what value of AF resulted in correlation for the failure load in the sand layer and the test set. Once a value of AF was determined points on the curves in Figures (14) through (18) were computed. No correlation, except for the load in sand layers and the total load on the H-pile, can be obtained.

The amount of dynamic increase in soil resistance resulting from the use of the point and side damping constants is entirely dependent upon velocity in equations (30) and (31) with the amount of this increase being unlimited.

Forehand and Reese pointed out that the static resistance of soil,  $R_s$ , and the dynamic resistance,  $R_d$ , can be related as shown by

$$R_d = R_s (1 + Jv) \quad (37)$$

If the dynamic resistance is 40% greater than the static resistance, as stated by Seed and Lundgren, and J is taken as .15 then

$$1.4 R_s = R_s (1 + .15V) \quad (38)$$

and  $V = 2.24 \text{ ft/sec.}$



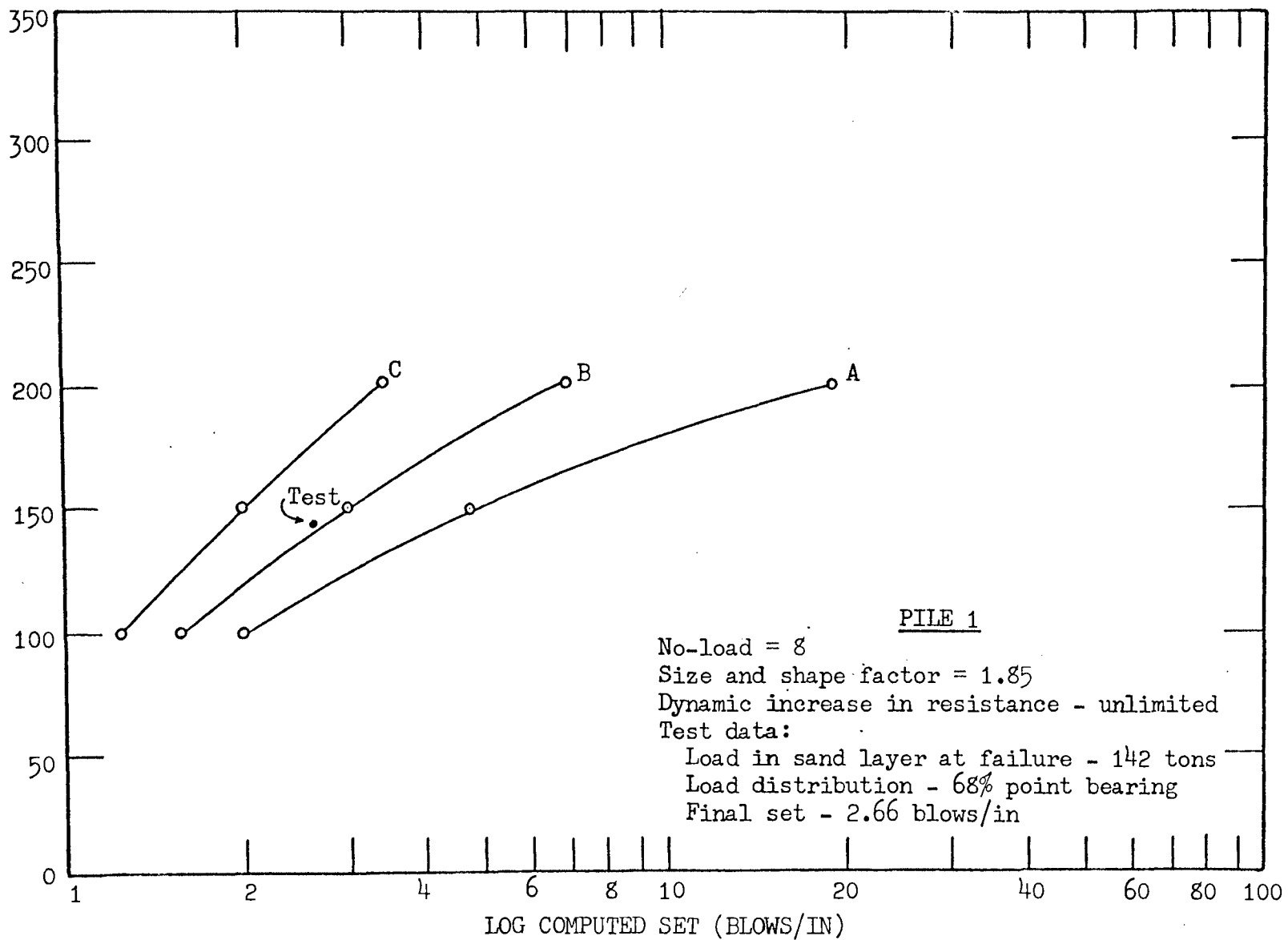


FIGURE 14. RESISTANCE - LOG COMPUTED SET

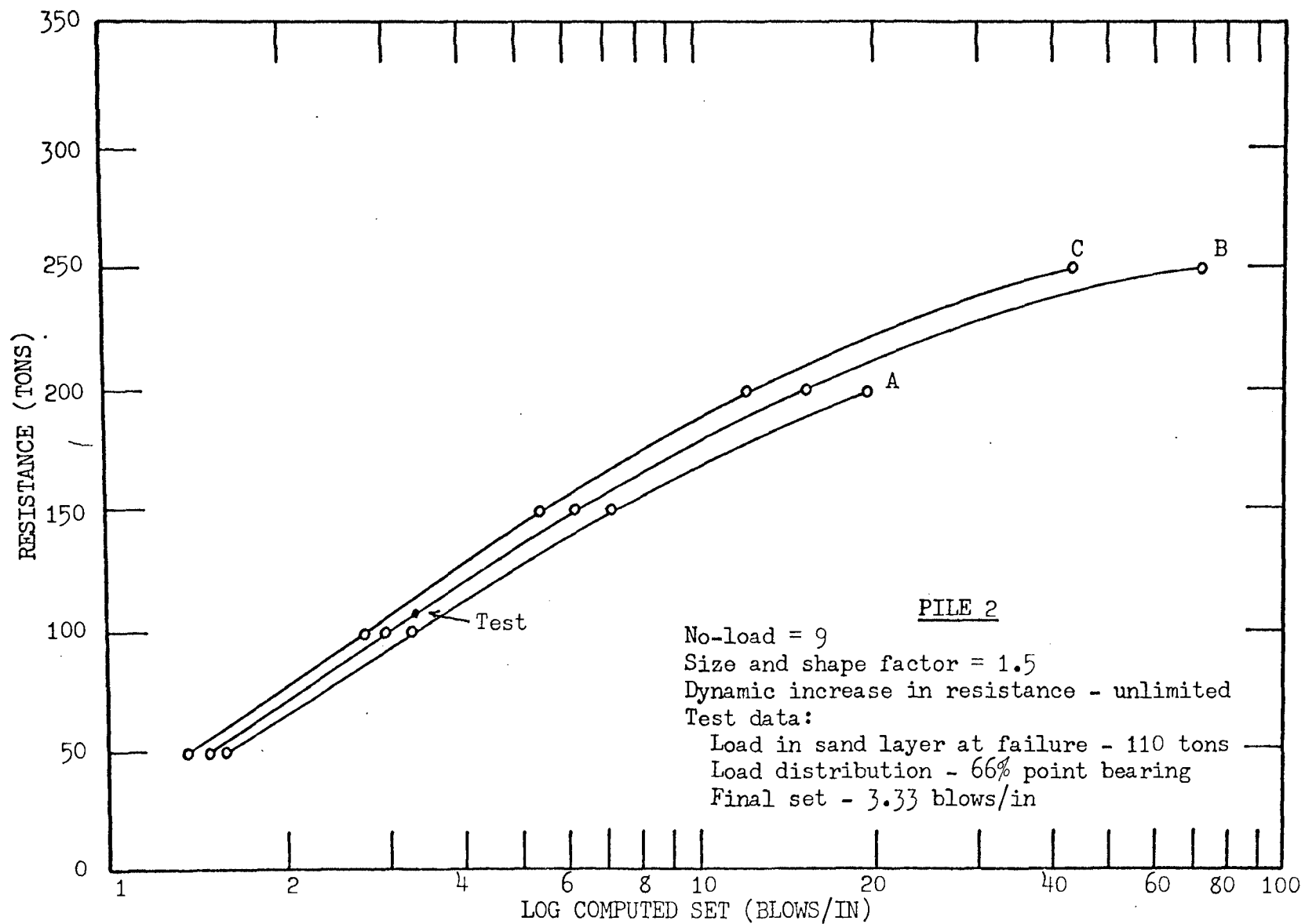


FIGURE 15. RESISTANCE - LOG COMPUTED SET

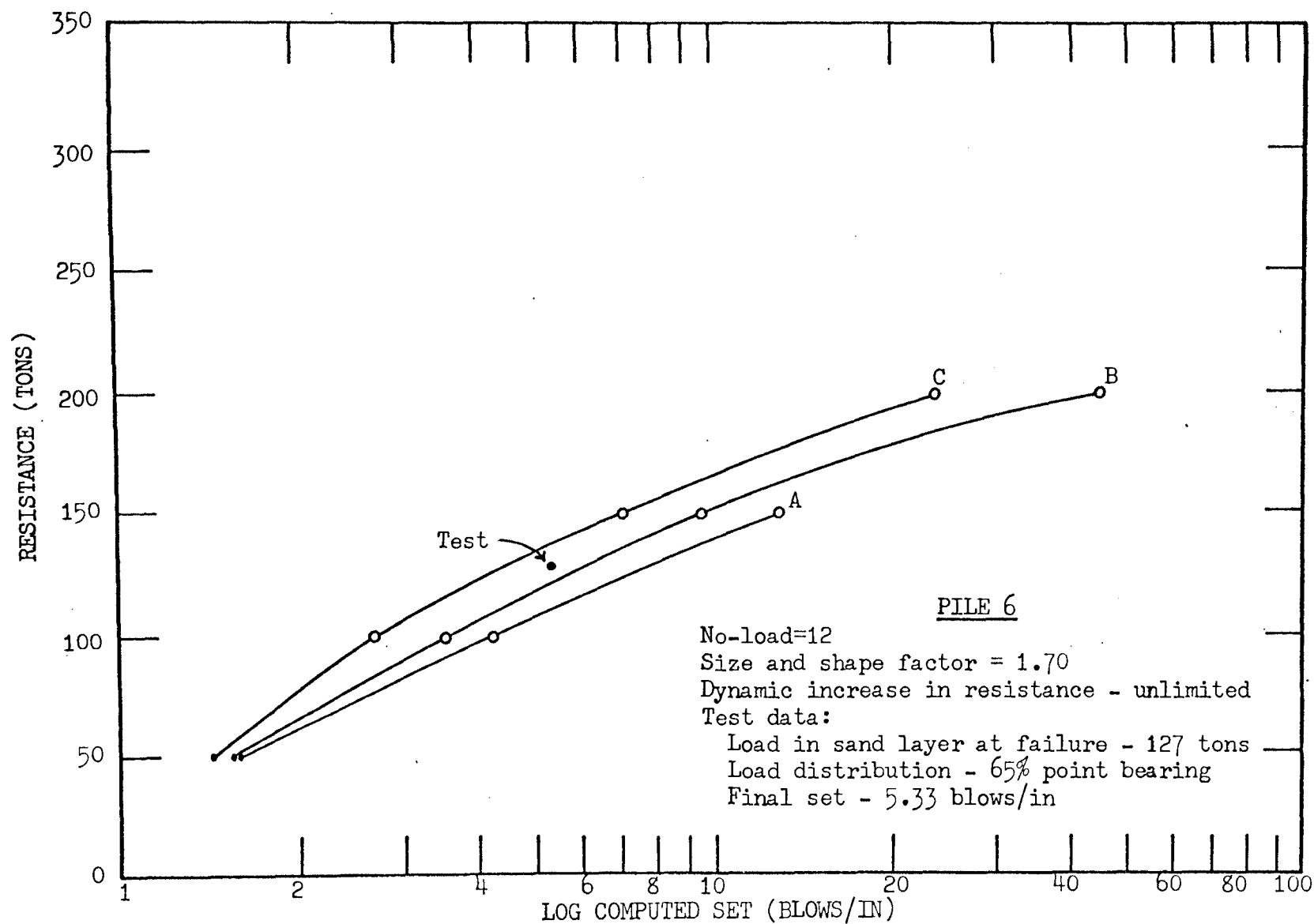


FIGURE 16. RESISTANCE - LOG COMPUTED SET

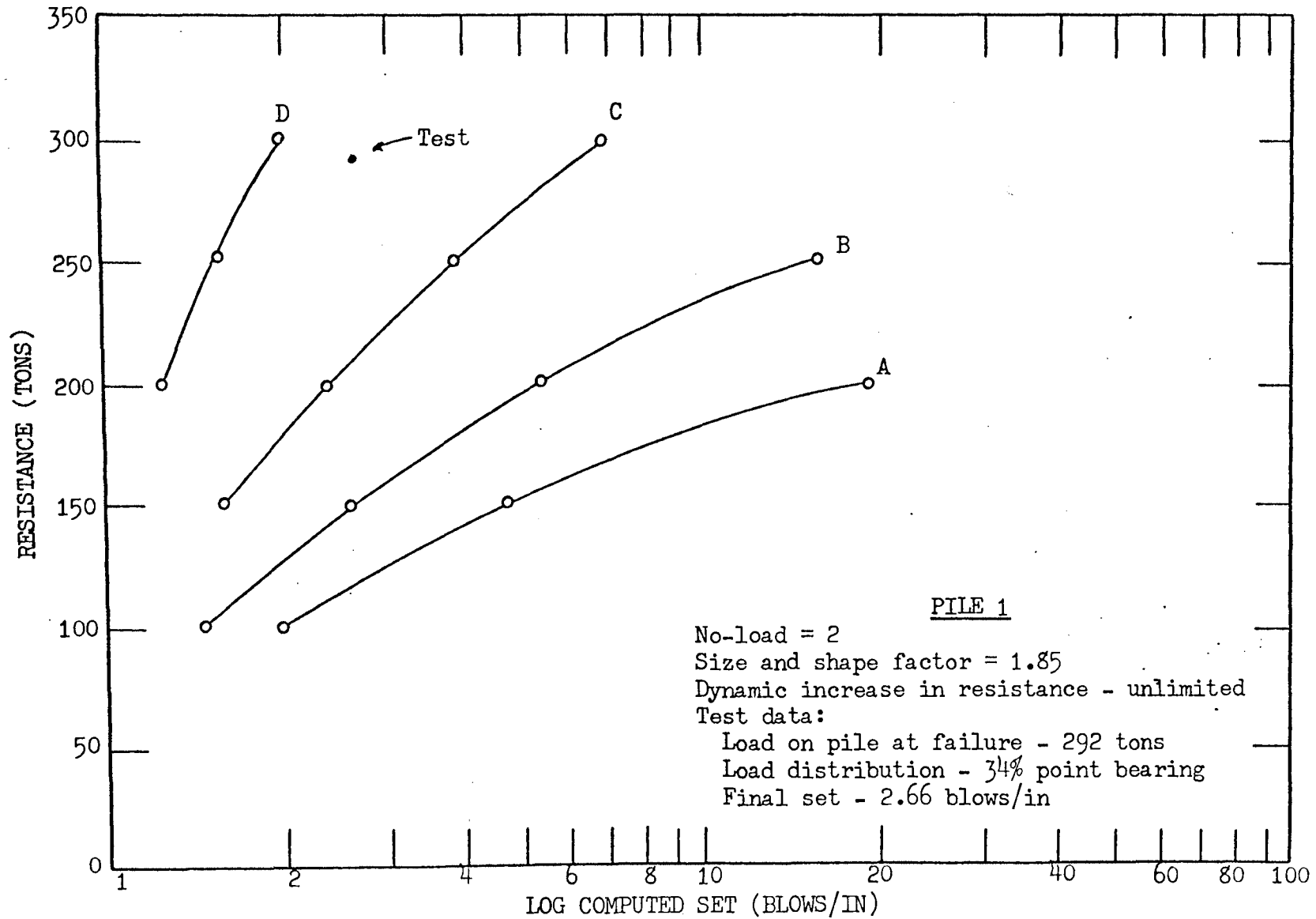


FIGURE 17. RESISTANCE - LOG COMPUTED SET

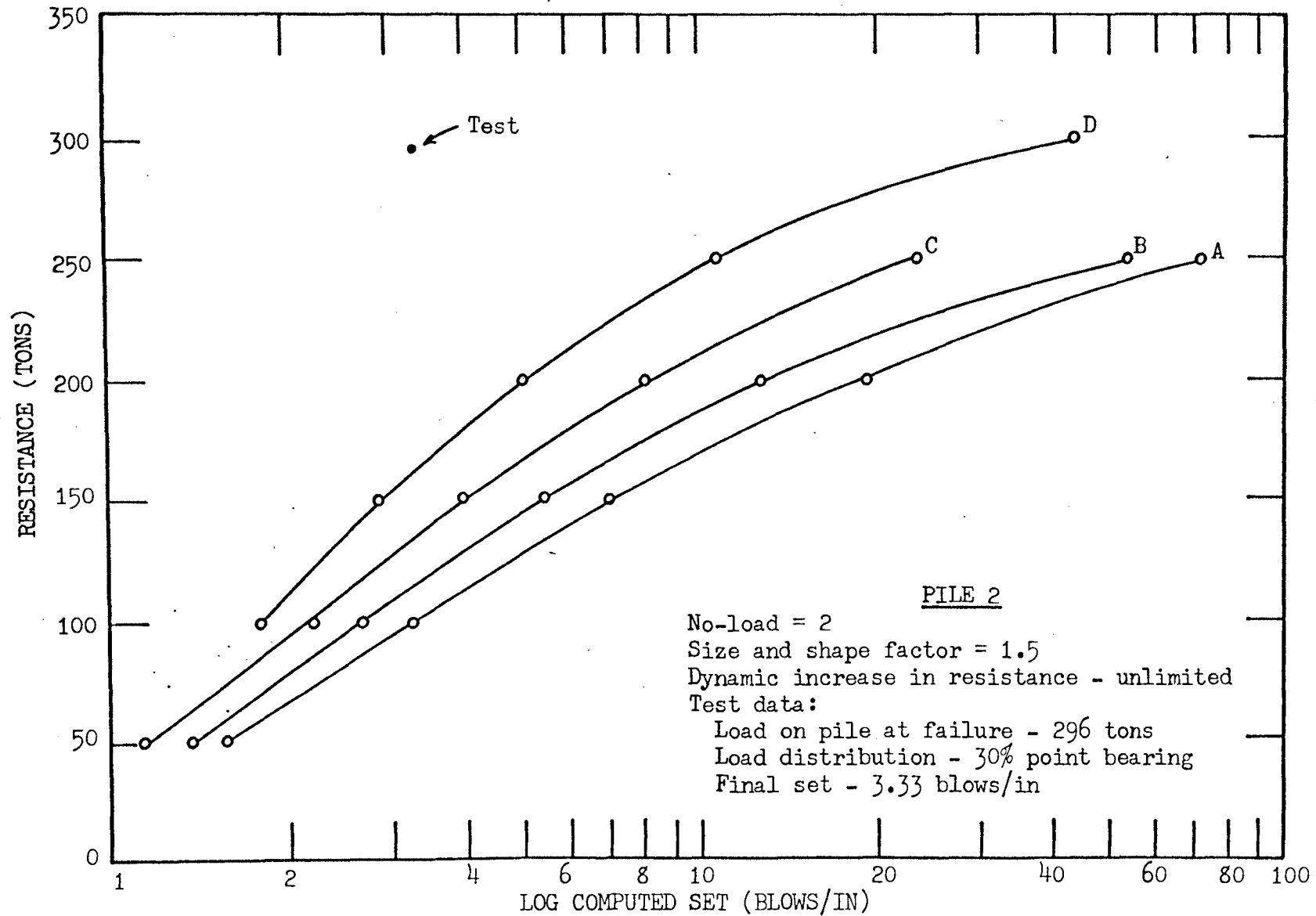


FIGURE 18. RESISTANCE - LOG COMPUTED SET

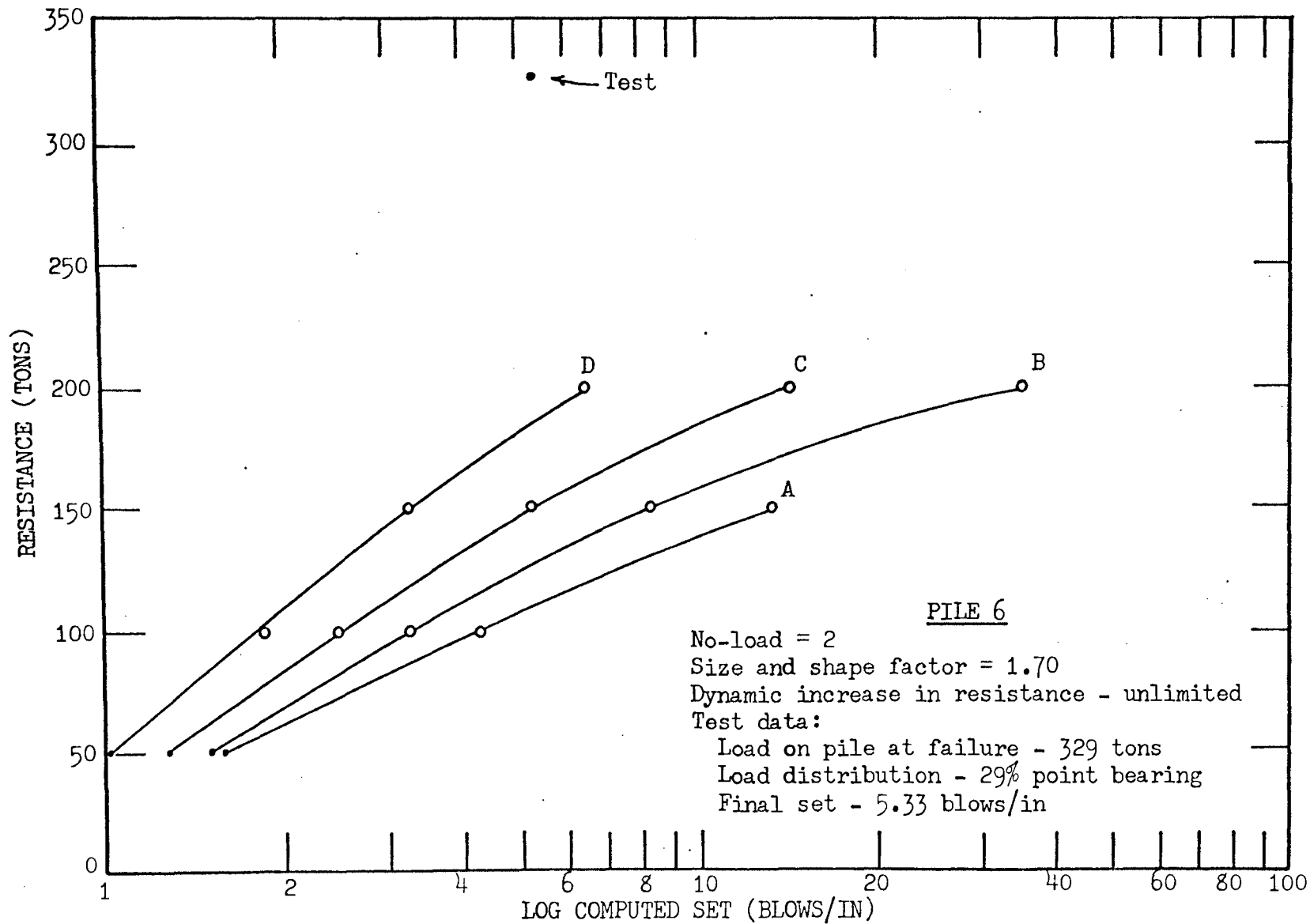


FIGURE 19. RESISTANCE - LOG COMPUTED SET

At a velocity of 2.24 ft/sec the soil resistance has increased the maximum of 40% assumed, but from solution of Smith's equations, the instantaneous velocity of the pile point may reach 10 ft/sec or higher. At this velocity if the point damping factor is taken as .15, the dynamic resistance at the point will be 250% greater than the static resistance.

In view of the findings of Seed and Lundgren, and Whitman it appears that a limit should be placed upon the dynamic increase in soil resistance. A limit is indicated even though the limitations were found to be applicable in triaxial compression tests rather than specifically to the dynamic penetration of piles. The resistance increasing terms  $(1 + Jv)$  and  $(1 + J^2v)$  of equations (35) and (36) have been changed to provide for this limit, with the amount of increase in the static resistance due to dynamic penetration being set at 40% for the point and 13% along the sides. The resistance will now increase with increased penetration and velocity to the maximum dynamic value shown as  $R'$  in Figure 1.

The searching procedure was again followed to determine a value of AF that gives correlation for the sand layer at the final driving resistance. As a result points on the curves in Figures (19) through (25) were computed.

Correlation for the pipe pile is obtained for the total pile (Figures 24 and 25) when the set used is 5-6 times the final driving set. Correlation for the H pile (Figure 23) is obtained when the final driving set is used.

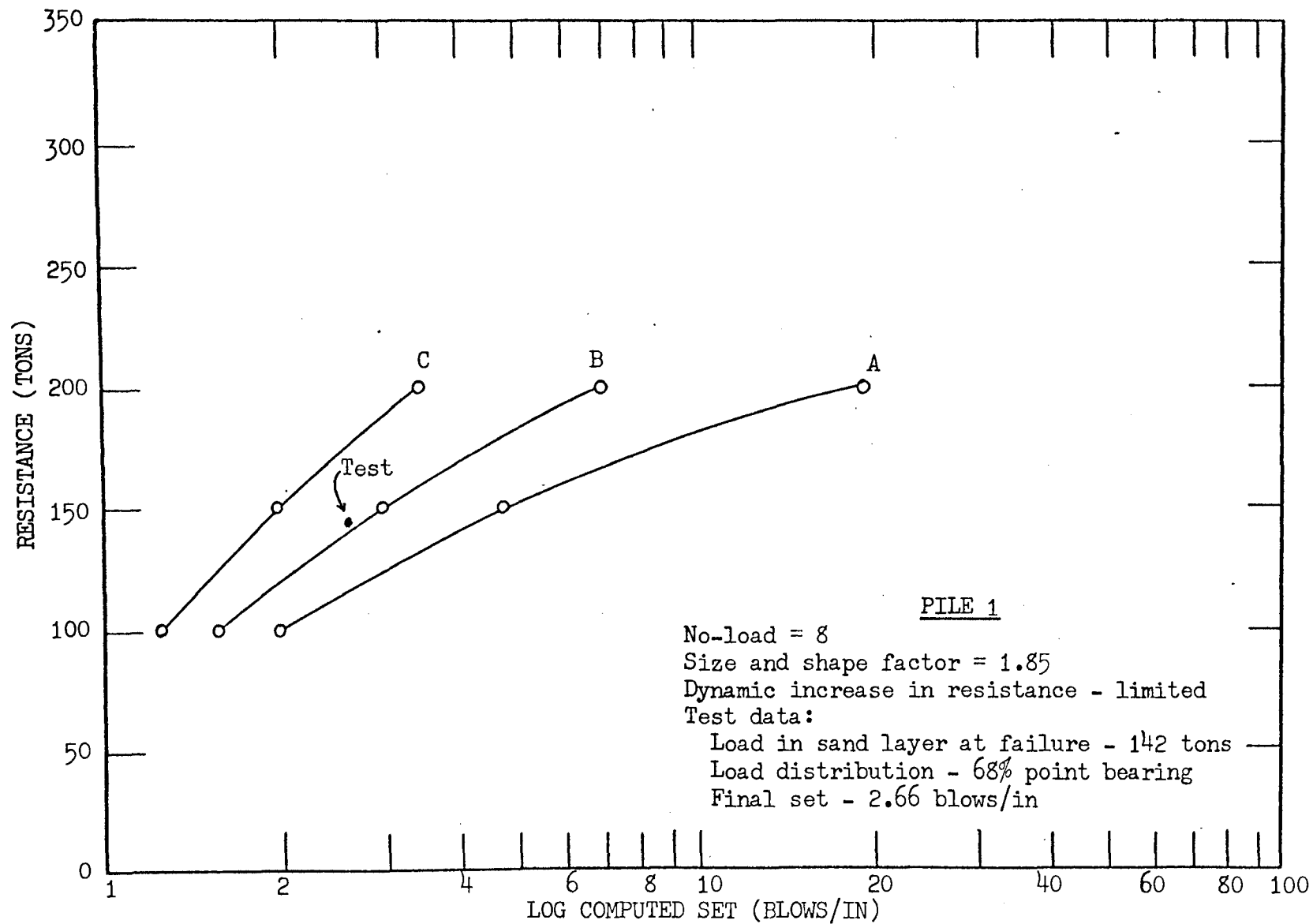


FIGURE 20. RESISTANCE - LOG COMPUTED SET



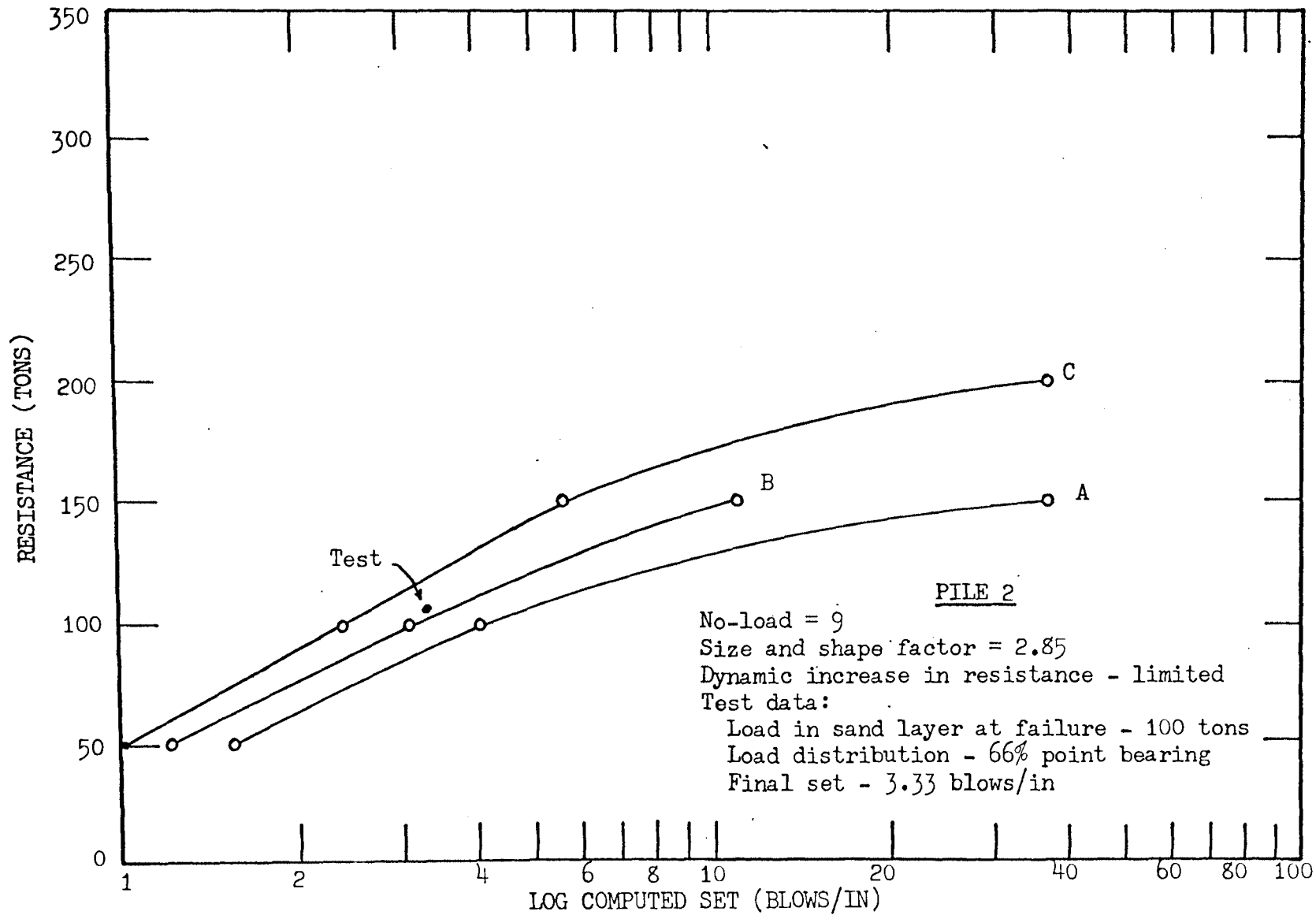


FIGURE 21. RESISTANCE - LOG COMPUTED SET

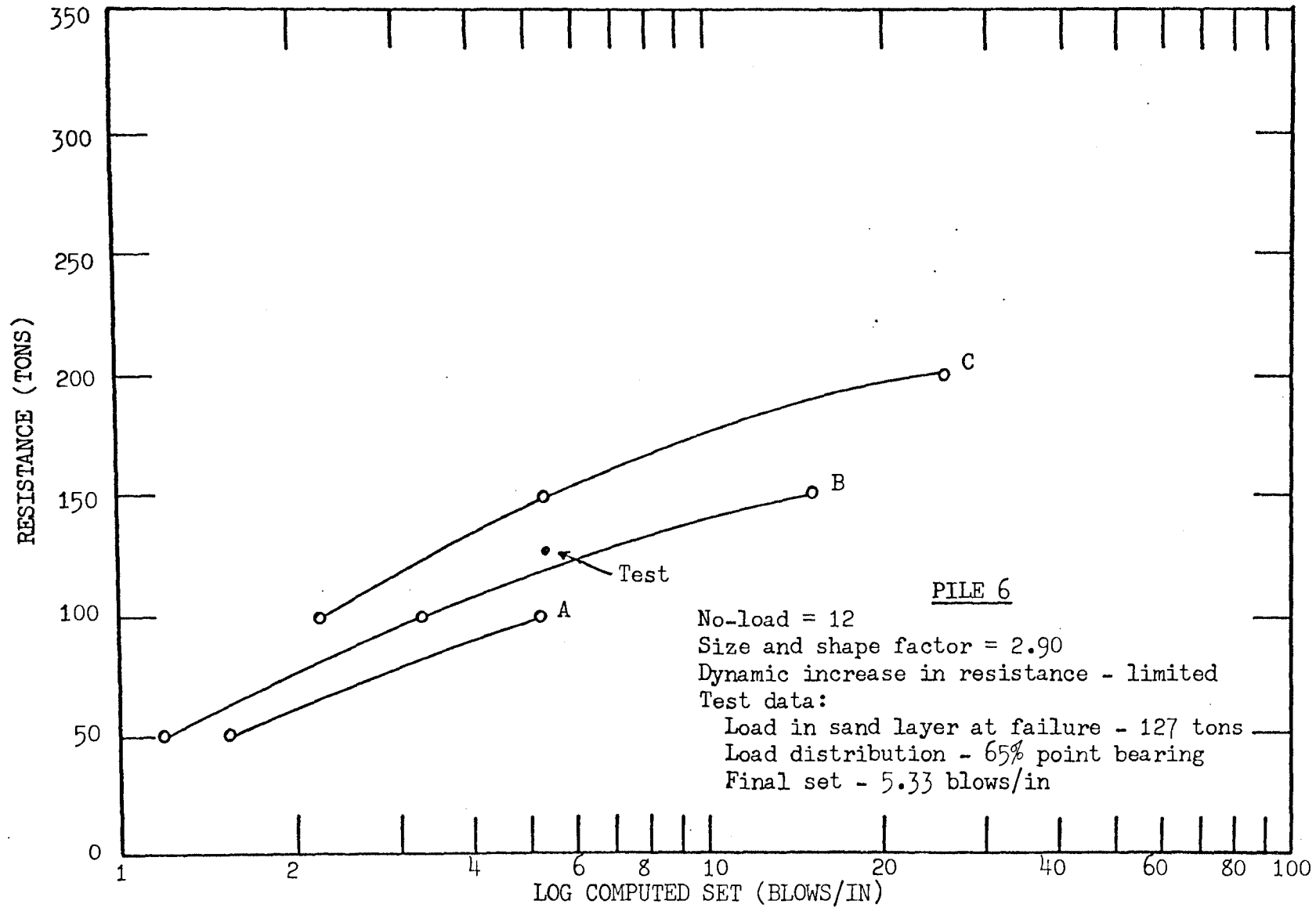


FIGURE 22. RESISTANCE - LOG COMPUTED SET

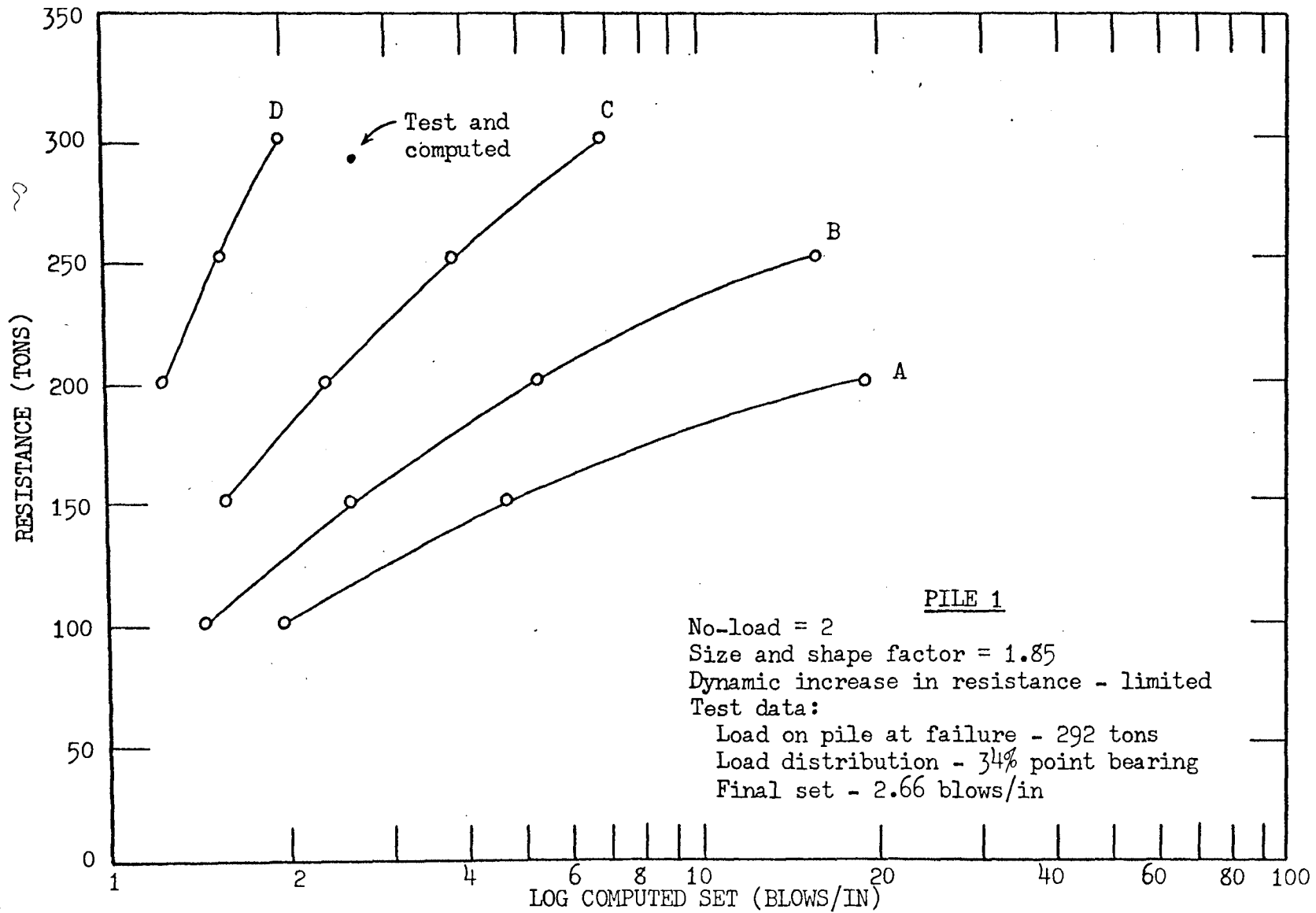


FIGURE 23. RESISTANCE - LOG COMPUTED SET

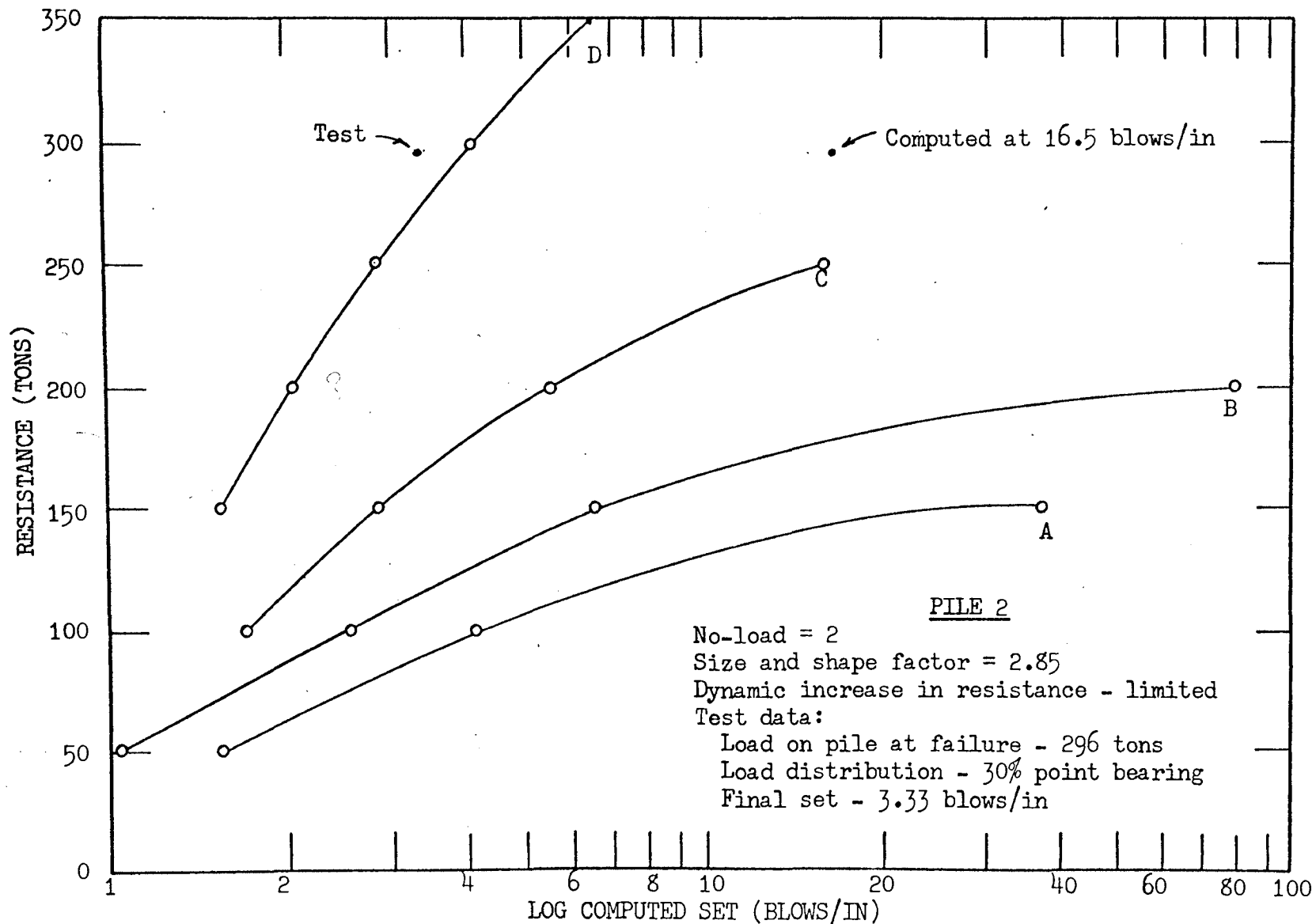


FIGURE 24. RESISTANCE - LOG COMPUTED SET

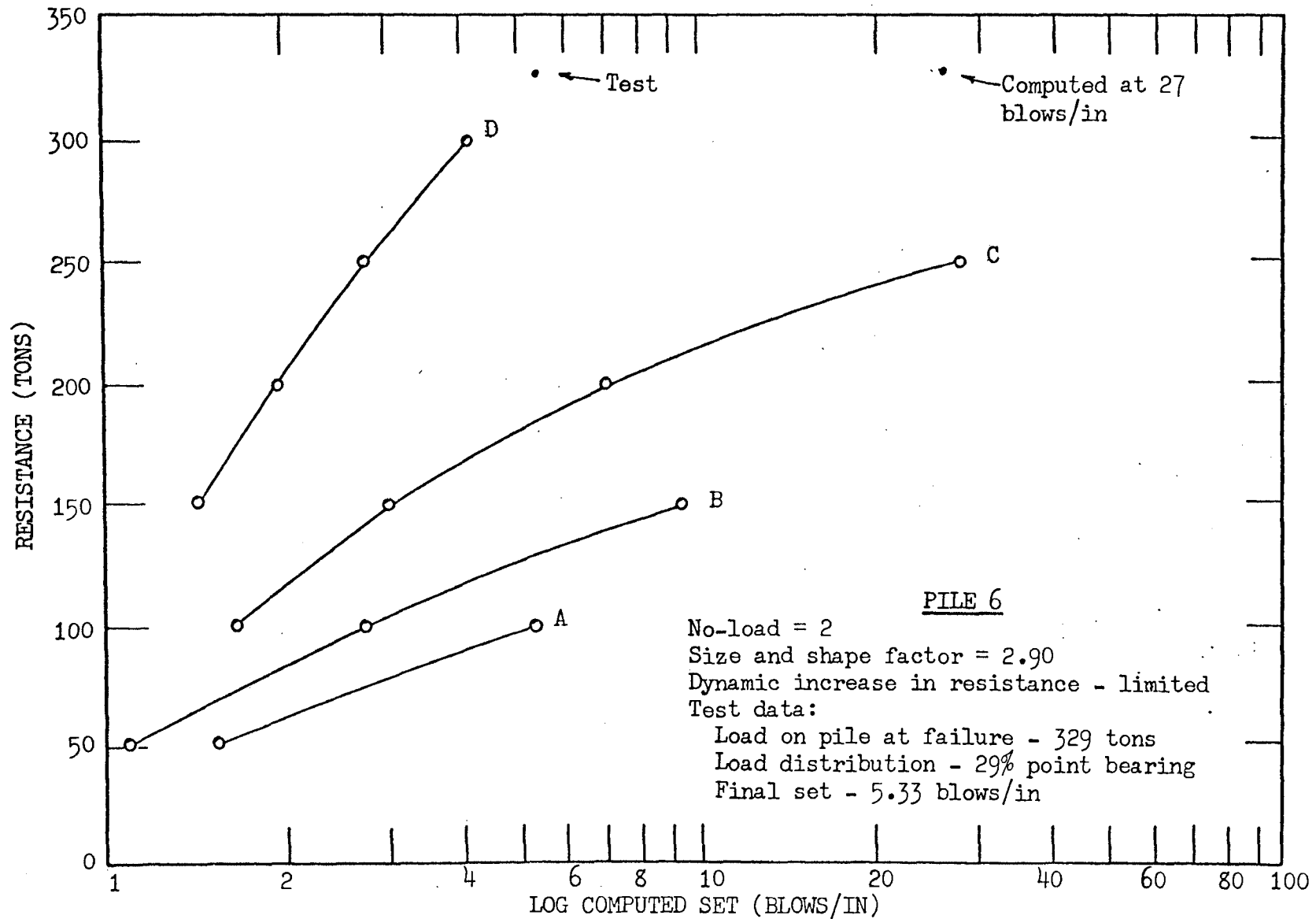


FIGURE 25. RESISTANCE - LOG COMPUTED SET

## IV. CONCLUSIONS

The procedure developed by Smith, with certain modifications, closely duplicates actual conditions that develop when a pile imbedded in soil has been struck by a hammer. These modifications account for the effect of cross-sectional size and shape of the pile and the limitation on the dynamic increase in soil resistance. The addition of these modifications create a more accurate and realistic analogy. When this modified procedure is used in conjunction with Yang's method for altering the final driving resistance a more accurate correlation can be obtained between observed and computed bearing capacities for the pipe piles. This is evident by the correlation for the piles in the sand layer. Correlation was not obtained between the observed and computed bearing capacity for the H-pile when Yang's method was used in conjunction with the modified procedure. However correlation was obtained without the use of Yang's method. This indicates that the equilibrium resistance of this pile shape is very nearly the same as the final driving resistance.

Before the wave equation method of evaluating the bearing capacity of a pile can be used as a reliable design procedure, studies must be made to determine the value of factors involved in the size and shape of the pile and dynamic increase in soil resistance. These values should be determined for all combinations of hammers, piles and soils. The values could be ascertained empirically by studying a sufficient number of piles for which adequate test data is available

(Appendix B), or by model testing in the laboratory. Both can be expressed as a function of the relative density of Sands, therefore, a normal soil investigation would provide all the soil information necessary.

At the present time the wave equation method of pile bearing capacity evaluation used in conjunction with an understanding of the soil conditions encountered in the field is more reliable than other existing pile formulas.

This and previous studies on the wave equation method of pile bearing capacity determination indicate that this method can be a useful tool in foundation engineering. However, a considerable amount of study, research and correlation on the method must be accomplished before it can be used with confidence on routine projects.

## BIBLIOGRAPHY

1. SMITH, E. A. L. (1962) Pile-driving analysis by the wave equation. Transactions of the American Society of Civil Engineers, Vol. 127 (1962), p. 1145.
2. FOREHAND, P. W. and REESE, J. L. (1963) Pile driving analysis using the wave equation. Thesis, Princeton University.
3. GATES, M. (1962) Discussion of pile driving analysis by the wave equation by E. A. L. Smith. Transactions of the American Society of Civil Engineers, Vol. 127 (1962), p. 1174.
4. JUNIKIS, A. R. (1962) Soil mechanics. D. Van Nostrand, New York, 791 p.
5. CUMMINGS, A. E. (1940) Dynamic pile driving formulas. Journal of the Boston Society of Civil Engineers, (January 1940), Vol. 27, n 1, p. 6-27.
6. SMITH, E. A. L. (1955) Impact and longitudinal wave transmission. Transactions of the American Society Mechanical Engineers, (August 1955), Vol 77, n 6, p. 963-973.
7. SEED, H. B. and LUNDGREN, R. (1954) Investigation of the effect of transient loading on the strength and deformation characteristics of saturated sands. Proceedings of the A.S.T.M., Vol 54 (1954), p. 1288.
8. WHITMAN, R. V. and HEALY, K. A. (1963) Shear strength of sands during rapid loadings. Transactions of the American Society of Civil Engineers, Vol 128 (1963), p. 1553-1586.
9. SELIG, E. T. and McKEE, K. E. (1961) Static and dynamic behavior of small footings. Journal of the Soil Mechanics and Foundation Division. Proceedings of the A.S.C.E. (December 1961), Vol 87, No. SM6, p. 29-47.
10. MANSUR, C. I. and KAUFMAN, R. I. (1956) Pile tests, low sill structure, Old River, La. Journal of the Soil Mechanics and Foundation Division. Proceedings of the A.S.C.E. (October 1956), Vol 82, No. SM4, p. 1079-1-33.



11. CHELLIS, R. D. (1961) *File foundations*. 2nd ed. New York, McGraw-Hill, 704 p.
12. YANG, N. C. (1956) Redriving characteristics of piles. *Journal of the Soil Mechanics and Foundations Division. Proceedings of the A.S.C.E.* (July 1956), Vol 82, No. SM3, p. 1026-1-19.

## APPENDIX A

## LIST OF SYMBOLS

- A = cross-sectional area of the pile material
- A<sup>o</sup> = cross-sectional area of the pile cap
- A<sub>e</sub> = effective cross-sectional area of the pile
- AF = pile size and shape factor
- a = velocity of the stress wave in an elastic rod
- C = a coefficient to increase soil resistance due to dynamic penetration
- C<sub>1</sub> = assumed elastic compression of the pile cap, in the Hiley Formula
- C<sub>2</sub> = assumed elastic compression of the pile, in the Hiley Formula
- C<sub>m</sub> = compression of spring m in time interval n
- c<sub>m</sub> = compression of spring m in time interval n-1
- D<sub>m</sub> = displacement of weight m, measured from its initial position, in time interval n
- D<sub>p</sub> = displacement of the pile point in time interval n
- D<sup>o</sup><sub>m</sub> = plastic displacement of the soil at weight m in time interval n
- D<sup>o</sup><sub>p</sub> = plastic displacement of the soil at the pile point in time interval n
- d<sub>m</sub> = displacement in weight m in time interval n-1
- dt = time interval
- E = modulus of elasticity of the pile material

- $E^*$  = modulus of elasticity of the pile cap material  
 $E_L$  = energy losses due to the elastic compressions of the pile and soil  
 $e$  = coefficient of restitution  
 $F_m$  = force exerted by spring  $m$  in time interval  $n$   
 $h$  = height of fall of the hammer or ram  
 $J$  = viscous damping coefficient for the soil resisting penetration of the pile point  
 $J^*$  = viscous damping constant for the soil along the sides of the pile  
 $K_1$  = energy losses due to impact  
 $K_m$  = spring constant for spring  $m$   
 $K_p$  = coefficient of passive earth pressure  
 $K_m^*$  = spring constant applicable to the soil at weight  $m$   
 $K_p^*$  = spring constant for the soil at the pile point  
 $k$  = factor in the Engineering News Formula that accounts for elastic compressions  
 $L$  = length of the pile  
 $L^*$  = length of the pile cap  
 $m$  = subscript denoting a particular weight of the mathematical model  
 $n$  = present time interval  
 $P$  = weight of the pile  
 $Q$  = amount of elastic compression of soil  
 $R$  = ultimate bearing capacity or resistance  
 $R^*$  = maximum dynamic resistance to penetration

- $R_d$  = dynamic resistance of the soil, varies from  $R_s$  to  $R^*$   
 $R_f$  = frictional resistance along the sides of the pile  
 $R_m$  = resistance applicable to weight  $m$  in time interval  $n$   
 $R_p$  = resistance of the soil to the penetration of the point  
 $R_s$  = static resistance of the soil  
 $s$  = penetration per blow for the last 6 inches  
 $t$  = time  
 $U$  = perimeter of the pile  
 $V$  = velocity of the hammer at the instant of impact  
 $V_m$  = velocity of weight  $m$  in time interval  $n$   
 $v_p$  = velocity of the pile point in the previous time interval  $n-1$   
 $W$  = weight of the hammer or ram  
 $Z_m$  = net accelerating force acting on weight  $m$  in time interval  $n$   
 $\gamma$  = unit weight of soil  
 $\epsilon$  = base of the natural logarithm  
 $\mu$  = coefficient of friction between the soil and pile  
 $\sigma_{max}$  = maximum stress at the fixed end of an elastic rod struck on the opposite end  
 $\phi$  = internal angle of friction  
 $\rho$  = mass per unit volume

## APPENDIX B

## RECOMMENDED PILE TEST PROGRAM

In order to thoroughly and accurately investigate the evaluation of pile bearing capacity by the use of the wave equation the following information from a pile driving and test program is required:

1. sufficient soil investigations so that a proper interpretation of soil conditions can be made,
2. weight of the hammer,
3. height of fall or rated energy of the hammer,
4. efficiency of the pile driving equipment,
5. length and cross-sectional area of the hammer,
6. cross-sectional area and type of material making up the cap block and cushion block so that restitution values can be determined,
7. length, cross-sectional area, and weight of the pile cap,
9. the following for the pile:
  - a. composition,
  - b. length,
  - c. embedded length,
  - d. weight,
  - e. cross-sectional dimensions for other than standard piles,
10. driving resistances encountered, especially the final driving resistance,
11. driving resistances after the soil has come to equilibrium,
12. load settlement relationships and the failure load,

13. load distribution between point bearing and side friction and distribution of side friction along the length of the pile as determined from strain gauges, and

14. stresses in the pile during driving.

Once a sufficient number of investigations are carried out to establish reliable values for the soil factors involved then only the information outlined in items 1 through 12 would be required to effectively evaluate the bearing capacity of a single pile.

APPENDIX C  
THE COMPUTER PROGRAM

The program for computing points of the resistance-log set curves is listed completely at the end of this appendix for the benefit of others who wish to do further investigation on the wave equation method. The program is the "Vary RU" program presented by Forehand and Reese (2) with minor modifications for use on an IBM 1620 Model II computer. The pile size and shape factor and the 40% limitation on the dynamic increase in soil resistance are also included in the program. The time required for the computer to compute one point is from 1 to 5 minutes depending upon the amount and distribution of the resistance. The spacing of the typed program corresponds to a 72 column data card with the C in the first line being in Column 1.

Preparation of the input data, except for the form and placement of the data on the card, which is given in the program; is accomplished as follows:

CARD ORDER	INFORMATION	DESCRIPTION
1	NCASE	Case number
2	ITURN	Indicates whether or not another set of data follows, +1, yes -1, no.
3	AREA 1, 2, & 3	Cross-sectional area of pile material at top, center and tip of the pile ( $\text{in}^2$ ).

4	M,IM1	Number of weights in the mathematical model and the number of weights less 1.
5	T	Time interval to be used in seconds.
Next M cards	W(I)	Weight of each weight (lbs).
Next M-1 cards	S(I)	Spring constants for the pile cap and pile weights (lbs/in).
Next M cards	SP(I)	Soil spring constants for all weights, initially zero.
Next card	RES1	Coefficient of restitution of the pile cap.
Next card	RES2	Coefficient of restitution of the cushion block.
Next card	V	Velocity of ram at instant of impact (ft/sec).
Next card	Q	Value for the maximum elastic compression of the soil (in).
Next card	Z	Point coefficient of viscous damping.
Next card	ZP	Side coefficient of viscous damping.
Next card	CAP	Ability of the pile cap to carry tension, +1, yes, -1, no.
Next card	RUB	Presence of side friction, +1, yes, -1, no.
Next card	MUD	Side friction distribution, +1, triangular, -1, rectangular.
Next card	RU1, ADD	Initial ultimate resistance and amount to be added per cycle (lbs).



Next card	ICYCLE, NOLOAD	Number of times resistance is increased by ADD and number of weights for which movement is not resisted by the soil.
Next card	LA, LB, LC	Numbers that determine the distribution of resistance between point and side, LA, LB, LC = 1,5,1 will give curves A, B, C, D, and E, 2,4,1 will give curves B, C, and D, etc.
Next card	AF	Pile size and shape factor

```

C      WAVE EQUATION VARY RU
      DIMENSION DS( 20),DM( 20),DL( 20),VS( 20),VM( 20),VL( 20)
      DIMENSION DPSM( 20),DPSL( 20)
      DIMENSION S( 20),W( 20),DP(500),R( 20),SP( 20),CS( 20)
      DIMENSION CM( 20),CL( 20),FS( 20),FM( 20),FL( 20),DPSS( 20)
207  READ 27,NCASE,ITURN
      27  FORMAT (I10/I10)
      READ 71,AREA1,AREA2,AREA3
      71  FORMAT(3F10.4)
      READ 70,M,IM1,T,(W(I),I=1,M),(S(I),I=1,IM1)
      1  ,(SP(I),I=1,M),RES1,RES2,V,Q,Z,ZP,CAP,RUB
      70  FORMAT (2I4/F10.4))
      READ 604,MUD
604  FORMAT(I4)
      READ 72,RU1,ADD,ICYCLE,NOLOAD
      72  FORMAT (2F10.4/2I4)
      73  FORMAT (3I4/I4)
      READ 73,LA,LB,LC,IRES
      74  FORMAT (F10.4)
      READ 74,AF
      PUNCH 30,NCASE
      30  FORMAT (12H CASE NUMBER I5)
      PUNCH 28,(I,W(I),S(I),SP(I),I=1,M)
      28  FORMAT (5H DATA//58H      M                W                S

```

```

1          SP/(I4,3F20.2))
          PUNCH 29,RES1,RES2,ZP,Z,Q,V
29  FORMAT (36H COEF. OF REST. OF CAPBLOCK (RES1) = F4.2/
136H COEF. OF REST. OF PILECAP (RES2) = ,F5.2/36H SIDE DAMPING FACT
20R (ZP) =          ,F4.1/36H POINT DAMPING FACTOR (Z) =          ,
3F4.2/36H GROUND QUAKE (Q) =          ,F4.2/
436H INITIAL RAM VELOCITY (Y) =          F6.2)
          PUNCH 605,MUD
605  FORMAT (6H MUD = I6)
          PUNCH 31,T,CAP,RUB
31  FORMAT (36H TIME INTERVAL =          F8.6/
136H CAP =          F6.2/
236H RUB =          F6.2//)
          PUNCH 608,RU1,ADD,ICYCLE,NOLOAD
608  FORMAT (5H RU = E20.4, 10H      ADD = E20.4/9H ICYCLE = I6,
113H      NOLOAD = I6)
          PUNCH 609,LA,LB,LC
609  FORMAT (5H LA = I4,10H      LB = I4,10H      LC = I4)
          PUNCH 610,AF
610  FORMAT (29H AF =          F6.2)
          CHECK = 2.*V
777  CONTINUE
          RU=RU1
          DO 600 IAM = 1,ICYCLE
          ITEM=M.NOLOAD
          AITEM=ITEM

```

```
DO 602 J=LA, LB, LC
FMAX1=0.0
FMAX2=0.0
FMAX3=0.0
FTEN1=0.0
FTEN2=0.0
FTEN3=0.0
DO 500 I=1, 20
DS(I)=0.0
DM(I)=0.0
DL(I)=0.0
VS(I)=0.0
VM(I)=0.0
VL(I)=0.0
DPSM(I)=0.0
DPSL(I)=0.0
R(I)=0.0
SP(I)=0.0
CS(I)=0.0
CM(I)=0.0
CL(I)=0.0
FS(I)=0.0
FM(I)=0.0
FL(I)=0.0
500 DPSS(I)=0.0
DO 501 I=1, 500
```

```

501 DP(I)=0.0
    DS(1)=V*12.*T
    VS(1) =      V+(-DS(1)*S(1))*T*32.2/W(1)
    VS(2)=(DS(1)*S(1)*T*32.2/W(2)
    DM(1)=DS(1)+VS(1)*12.*T
    DM(2)=VS(2)*12.*T
    CM(2)=DM(2)
    VM(1)=VS(1)-((DM(1)-DM(2))*S(1))*T*32.2/W(1)
    VM(2)=VS(2)+((DM(1)-DM(2))*S(1)-(DM(2)-DM(3))*S(2))*T*32.2/W(2)
    VM(3)=VS(3)+((DM(2)-DM(3))*S(2)-R(3))*T*32.2/W(3)
    CM(1)=DM(1)-DM(2)
    AJ=J
    PART=(5.-AJ)/4.
    SP(M)=PART*RU/Q
    SIDE=RU-PART*RU
    LOAD=NOLOAD+1
    IF(MOD)650,651,652
650 DO 601 N=LOAD,IM1
601 SP(N)=SIDE/(AITEM*Q)
    SP(M)=SP(M)+SIDE/(AITEM*Q)
    GO TO 651
652 DO 603 N=3,IM1
    NT=N-2
    NT1=2*NT-1
    IM2=N-2
    ANT1=NT1

```

```
AIM2=IM2
603 SP(N)=SIDE*ANT1/((AIM2**2)*Q)
    SP(M)=SP(M)+SIDE*(2.*AIM2-1.)/((AIM2**2)*Q)
651 CONTINUE
    DO 101 N=3,500
        MLESS1=M-1
        DO 130 I=1,M
130  DL(I)=DM(I)+VM(I)*12.*T
        DO 131 I=1,MLESS1
131  CL(I)=DL(I)-DL(I=1)
        13 IF(DL(M)) 12,12,14
        12 DE=0.0
            GO TO 24
        14 IF(DL(M)-Q) 16,16,18
        16 DE=0.0
            GO TO 24
        18 VALUE=DL(M)-Q
            IF(VALUE-DE) 22,22,20
        20 DE=VALUE
            GO TO 24
        22 DE=DE
        24 DP(N)=DE
            TUB=(1.+VL(M)*Z)
            IF(1.4-TUB) 51,52,52
        51 TUB=1.4
        52 CONTINUE
```

```
R(M)=(DL(M)-DP(N))*SP(M)*TUB*AF
IF(DP(N)) 25,25,26
26 IF(DP(N)-DP(N-1)) 197,197,25
25 CONTINUE
3 VAL=S(1)*CL(1)
IF(CL(1)-CM(1)) 5,5,4
4 FL(1)=VAL
GO TO 33
5 CL(1)=CM(1)
FL(1)=VAL/(RES1**2)-(1./(RES1**2)-1.)*S(1)*CL(1)
33 VAL2=S(2)*CL(2)
IF(CL(2)-CM(2)) 35,35,34
34 FL(2)=VAL2
GO TO 37
35 CL(2)=CM(2)
FL(2)=VAL2/(RES2**2)-(1./(RES2**2)-1.)*S(2)*CL(2)
37 IF(CAP) 38,36,36
38 IF(FL(2)) 39,36,36
39 FL(2)=0.0
36 CONTINUE
7 IF(FL(1)) 8,133,133
8 FL(1)=0.0
133 DO 132 I=3,MLESS1
132 FL(I)=CL(I)*S(I)
IF(FL(2)) 213,211,210
213 IF(FTEN1-FL(2)) 211,211,214
```

```
214 FTEN1=FL(2)
    GO TO 211
210 IF(FMAX1-FL(2)) 215,211,211
215 FMAX1=FL(2)
211 CONTINUE
    MC=M/2+1
    IF(FL(MC)) 216,217,218
216 IF(FTEN2-FL(MC)) 217,217,219
219 FTEN2=FL(MC)
    GO TO 217
218 IF(FMAX2-FL(MC)) 220,217,217
220 FMAX2=FL(MC)
217 CONTINUE
    IF(FL(IM1)) 221,222,224
221 IF(FTEN3-FL(IM1)) 222,222,223
223 FTEN3=FL(IM1)
    GO TO 222
224 IF(FMAX3-FL(IM1))225,222,222
225 FMAX3=FL(IM1)
222 CONTINUE
42 IF(RUB)49,49,44
44 DO 48 I=3,MLESS1
    DPSL(I)=DPSM(I)
    CHANGE=DL(I)-Q
    SUM=DL(I)+Q
    IF(DPSL(I)-CHANGE) 45,46,46
```



```
45  DPSL(I)=CHANGE
46  IF(DPSL(I)-SUM)48,48,47
47  DPSL(I)=SUM
    SUB=1.+(VM(I)*2P)
    IF(1.13-SUB) 53,54,54
53  SUB=1.13
54  CONTINUE
48  R(I)=(DL(I)-DPSL(I)*SP(I)*SUB
49  DO 50 I=1,M
    VL(I)=VM(I)+(FL(I-1)-FL(I)-R(I))*T*32.2/W(I)
50  CONTINUE
    DO 75 K=1,M
    X=1.
    IF(VL(K))      75,75,800
75  CONTINUE
    GO TO 199
800 CONTINUE
    IF(VL(2)-CHECK) 99,99,190
99  IF(VL(M)-CHECK) 102,102,194
102 DO 98 K=1,M
    DS(K)=DM(K)
    DM(K)=DL(K)
    DL(K)=0.0
    VS(K)=VM(K)
    VM(K)=VL(K)
    VL(K)=0.0
```

```
CS(K)=CM(K)
CM(K)=CL(K)
CL(K)=0.0
FS(K)=FM(K)
FM(K)=FL(K)
FL(K)=0.0
DPSS(K)=DPSM(K)
DPSM(K)=DPSL(K)
98  DPSS(K)=0.0
101 CONTINUE
    GO TO 196
190 PUNCH 191,N
191 FORMAT (64H VELOCITY OF PILE CAP EXCEEDED TWICE THE RAM VELOCITY W
1HEN N WAS I3)
    GO TO 196
194 PUNCH 195,N
195 FORMAT (64H VELOCITY OF PILE TIP EXCEEDED TWICE THE RAM VELOCITY W
1HEN N WAS I13)
    GO TO 196
197 PUNCH 198,N
198 FORMAT (26H DP BECAME CONSTANT AT N = 13)
    GO TO 196
199 PUNCH 200,N
200 FORMAT (52H ALL VL WERE SIMULTANEOUSLY NEGATIVE OR ZERO AT N = I4)
196 CONTINUE
    PUNCH 607,RU
```

```
607  FORMAT (27H ULTIMATE RESISTANCE (RU) = E15.4)
      BLOW = 1./DP(N)
      PUNCH 805,BLOW
805  FORMAT(66H
      1BLOWS/IN= E10.3)
602  CONTINUE
      RU=RU+ADD
600  CONTINUE
      IF(ITURN) 205,205,207
205  CALL EXIT
      END
```

## APPENDIX D

## INTERPRETATION OF RESISTANCE-LOG SET CURVES

In Figures 8 through 25 the curves labeled A, B, C, D represent computed results when 100, 75, 50 and 25% of the total resistance plotted on the ordinate is provided as point resistance. The remainder of the resistance is distributed along the length of the pile as side friction.

When "No Load = 8, 9 or 12," depending on whether the curves are for Piles 1, 2 or 6, movement of only that part of the pile penetrating the dense sand layer is resisted by the soil. When "No Load = 2" the movement of all but the top two weights of Figure 13 is resisted by the soil. The points labeled "Test" are the plots of the observed data obtained from the pile loading test and shown in the lower right hand corner of each figure. Only in Figures 14, 15, 16, 17, 20, 21, 22 and 23 do the "Test" points match completely the observed data shown on the respective figures.

The points labeled "Computed" are points plotted at the observed failure load and computed set. Correlation is obtained when this computed point is located with respect to curves A, B, C or D in accordance with the observed load distribution shown in the lower right hand corner of each figure.

In interpolating between curves A, B, C and D it must be remembered that the spread is nonlinear.

## VITA

Captain Stuart H. Williams was born January 12, 1937, in Detroit, Michigan. He received his elementary education in Erin Township, Macomb County, Michigan and his high school education in Mt. Clemens, Michigan. He received a Bachelor of Science Degree in Mining Engineering from the Michigan College of Mining and Technology in June, 1958.

He entered military service in May 1959 and has served in the United States and overseas in Korea. He has completed both the Engineer Officer Basic Course and the Engineer Officer Career Course conducted at Fort Belvoir, Virginia. He married Diane Peterson of Detroit, Michigan on October 10, 1959 and they have a daughter, Cheryl Lynn born September 18, 1964.

In May 1963 he was sent to the Missouri School of Mines and Metallurgy by the U. S. Army to obtain a Master of Science Degree in Civil Engineering. He received a Bachelor of Science Degree in Civil Engineering from the University of Missouri at Rolla in August, 1964 and has been enrolled in the Graduate School of the University of Missouri at Rolla since January, 1964.